
Adaptation in simple and complex fitness landscapes*

Kavita Jain¹ and Joachim Krug^{1,2}

1. Institut für Theoretische Physik, Universität zu Köln, Germany

2. Laboratory of Physics, Helsinki University of Technology, Finland

kavita@thp.uni-koeln.de, krug@thp.uni-koeln.de

1 Introduction

The notion that evolution can be viewed as a hill-climbing process in an adaptive landscape was introduced in 1932 by Sewall Wright [1], and remains one of the most powerful images in evolutionary biology [2]. Since the discovery of the molecular structure of genes it has been clear that the substrate over which the adaptive landscape should be properly defined is the space of genetic sequences [3]. Nevertheless, apart from a few landmark papers [4, 5], adaptation has not been in the focus of the theory of molecular evolution, which instead has concentrated on the effects of stochastic drift in a neutral (*flat*) fitness landscape [6]. This situation is presently changing [7, 8]. Long-term evolution experiments on microbial populations [9] are beginning to produce a wealth of data, on the phenotypic as well as on the genotypic level, which make it meaningful to ask precise questions about the timing and size of adaptive events, and what they can tell us about the structure of the underlying adaptive landscape.

In this chapter we introduce a class of sequence-based models of adaptation, which have been the subject of much recent interest in theoretical population genetics as well as in biologically inspired statistical physics. These models describe the behavior of a population of haploid, asexual individuals, each characterized by a genetic sequence of fixed length, in an adaptive landscape which assigns a fitness value to each genotype. The population is exposed to the competing influences of *mutations*, which tend to increase the genetic variability, and *selection*, which focuses the population in regions of high fitness. The dynamics is deterministic, which implies that the genetic drift induced by the stochastic sampling noise in finite populations is neglected, and the adaptive landscape is generally taken to be time-independent. In view of

* To appear in *Structural approaches to sequence evolution: Molecules, networks and populations*, ed. by U. Bastolla, M. Porto, H.E. Roman and M. Vendruscolo (Springer, Berlin 2006).

the vastness of the field, the selection of topics is unavoidably biased by the interests and preferences of the authors. For a more comprehensive coverage we refer the reader to several recent review articles [10, 11, 12, 13, 14].

The chapter is organised as follows. In the next section the key concepts and their mathematical representation are introduced, and several types of mutation-selection dynamics are described, leaving the form of the adaptive landscape unspecified. In Sect. 3 we consider simple fitness landscape comprising a single adaptive peak or possibly two competing peaks. Here the central theme is the *error threshold* phenomenon, which refers to the sudden delocalization of the population from the fitness peak as the mutation rate increases beyond a critical value. As is described in this book in the chapter by Ester Lázaro, the error threshold and the related concept of a *quasispecies* play an important role in the population dynamics of RNA viruses and in the development of antiviral strategies. Due to its similarity to a phase transition, the error threshold has been thoroughly analyzed using a range of methods from statistical physics. We give an elementary derivation of the critical mutation rate, and describe several modifications of the basic model, including fitness peaks with a variable amount of epistasis, diploid populations, semiconservative replication, and time-dependent landscapes.

Section 4 is devoted to complex fitness landscapes consisting of many peaks and valleys. Such landscapes can be modeled by ensembles of random functions, which links this subject to the statistical physics of disordered systems. Whereas so far the discussion has been restricted to static or steady state properties, time-dependent aspects of mutation-selection dynamics are discussed in Sect. 5. Finally, experimental realizations (*in vitro* as well as *in vivo*) of the models are described in Sect. 6, and some concluding remarks are presented in Sect. 7.

2 Basic concepts and models

In the following discussion, the constituents of a population carry a string $\sigma \equiv \{\sigma_1, \dots, \sigma_N\}$ where each of the N letters σ_i is taken from an alphabet of size $\ell \geq 2$. In classical population genetics, σ represents the configuration of alleles (variants of a gene) σ_i located at gene loci i . Typically, one-locus, ℓ allele models where ℓ can take values between two (wild type and mutant) to infinity (continuum of alleles) have been considered [15]. In the language of population genetics, we are here concerned with multilocus models with complete linkage [11].

At the molecular level, σ represents the genetic sequence of an individual. For DNA(RNA) based organisms, $\ell = 4$ corresponding to the nucleotide bases A, T(U), C and G and the sequence length N varies from a few thousands for viruses to about 10^9 for humans. Thus, the total number 4^N of sequences available is hyperastronomically large. The minimum value of $\ell = 2$ can be

obtained by lumping A and G together in purins and C, T and U in pyrimidines. The sequences may also represent proteins composed of a few hundred amino acids taken from an alphabet of size $\ell = 20$ [3].

2.1 Fitness, mutations, and sequence space

The essence of natural selection is that the relative reproductive success of an individual determines whether the corresponding genotype becomes more or less abundant in the population. The *fitness* of an individual is a quantitative measure of its reproductive success; depending on the context, it may be defined as the *viability* of an organism, i.e. the probability to survive to the age of reproduction [2], the replication rate of a microbe, the binding affinity of regulatory proteins to DNA [16] or of antibodies produced by B-cells to pathogens [17], the program execution speed for digital organisms [18], or the cost function in an optimization problem [19].

In principle, one should assign fitness to the phenotype which then should be related to the genotype; unfortunately, the genotype-phenotype map is complicated and largely unknown except for a few cases [20] (see also Sect. 4.1). This problem is usually outflanked by associating fitness $W(\sigma)$ with the genotype itself and define it to be *the expected number of offspring produced by an individual with sequence σ* [14]. This definition applies to the case of discrete generations, and is known as *Wrightian* fitness. To pass to continuous time dynamics we write

$$W(\sigma) = \exp[w(\sigma)\Delta t] \approx 1 + w(\sigma)\Delta t, \quad \Delta t \rightarrow 0, \quad (1)$$

where Δt is the generation time and $w(\sigma)$ is referred to as the *Malthusian* fitness [10]. For future reference we note that multiplication of the Wrightian fitnesses by a common factor implies a constant additive shift of the Malthusian fitnesses.

Organism	Genome size	Rate per base	Rate per genome
Bacteriophage $Q\beta$	4.5×10^3	1.4×10^{-3}	6.5
Vesicular Stomatitis virus	-	-	3.5
Bacteriophage λ	4.9×10^4	7.7×10^{-8}	0.0038
<i>E. Coli</i>	4.6×10^6	5.4×10^{-10}	0.0025
<i>C. Elegans</i>	8.0×10^7	2.3×10^{-10}	0.018
Mouse	2.7×10^9	1.8×10^{-10}	0.49
Human	3.2×10^9	5.0×10^{-11}	0.16

Table 1. Spontaneous mutation rates for various organisms taken from [21]. The first two organisms have RNA as genetic material and the rest are DNA based.

In the next subsection, we will discuss models in which *mutations* occur either as copying errors in the genetic material during cell division or induced

by some external influences. In Table 2.1, the spontaneous mutation rates for some organisms are shown. They differ by orders of magnitude between RNA-based viruses whose mutation rate per genome exceeds unity, and DNA-based organisms, which can afford the complex replication machinery needed to reduce the mutation rate to a much lower level. It has been suggested that the high mutation rate of RNA viruses, rather than being due to the lack of correction mechanisms, may constitute an adaptation to the rapidly fluctuating environments that these organisms encounter (see the chapter by E. Lázaro). Within the DNA organisms, the mutation rate per base is seen to decrease with increasing sequence length, and the mutation rate per genome is roughly constant for similar organisms. However, mutation rates per genome in higher eukaryotes become comparable to those of DNA-based microbes if referred to the *effective* genome size, which excludes non-coding regions [21].

Before we describe the mutation-selection models, we need to specify the space of sequences on which the evolutionary dynamics operate. The structure and geometry of the sequence space depends on the nature of the allowed moves that change one sequence into another. In the simplest case of a genome of fixed length N subject only to point mutations (which we will restrict ourselves to throughout this chapter), the natural choice for the sequence space is the Hamming space with ℓ^N points. Two sequences σ and σ' are separated by the Hamming distance $d(\sigma, \sigma')$ which is given by

$$d(\sigma, \sigma') = \sum_{i=1}^N (1 - \delta_{\sigma_i, \sigma'_i}). \quad (2)$$

The Hamming distance simply counts the number of letters in which the two sequences differ, that is, the number of point mutations needed to mutate σ into σ' (and viceversa). The Hamming space for $N = 3$ and $\ell = 2$ is shown in Fig. 1 (left). The sequences are located at the corners of a cube, which for general N becomes the N -dimensional *hypercube*.

To give an example of a sequence space with a somewhat different geometry, we consider the Graph Bipartitioning Problem (GBP) [22] (see also Sect. 4.3). In the GBP, as the name suggests, the problem is to partition a graph with given connections into two sets A and B with equal number of vertices, such that the number of connections between A and B is minimised. A bipartitioning configuration is mapped onto a binary sequence by setting $\sigma_i = 1$ if the vertex i belongs to set A , and $\sigma_i = -1$ else. Thus the sequence space consists of those $\binom{N}{N/2}$ configurations σ for which $\sum_i \sigma_i = 0$, a subset of the Hamming space. An elementary move exchanges a pair of vertices between the sets A and B . Two configurations are said to be at a distance $d_{\text{GBP}}(\sigma, \sigma') = d$ if they can be related by d exchange moves, so that d_{GBP} is half of the Hamming distance defined above. The GBP sequence space for $N = 4$ is shown in Fig. 1 (right).

The Hamming space as well as the GBP sequence space are symmetric and regular graphs, in the sense that each vertex has the same number of neighbors

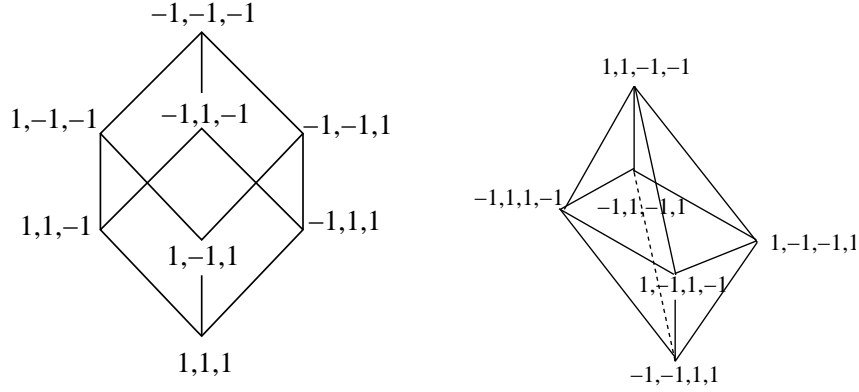


Fig. 1. Examples of sequence spaces. Left panel: Hamming space of binary sequences of length $N = 3$. Right panel: Graph bipartitioning problem space for $N = 4$. In both cases $\sigma_i = \pm 1$ and nearest neighbors are connected by lines.

and all vertices are equivalent. This is no longer true if mutations that change the sequence length through deletions, insertions or gene duplications are taken into account. Genetic recombination, which is of crucial importance for sexual reproduction, leads to additional complications, because it introduces moves which involve pairs of sequences [19].

We return to the case of point mutations acting on sequences of fixed length N , and proceed to derive an expression for the mutation probabilities taking one sequence to another. If the mutations change a letter σ_i to any one of the other $\ell - 1$ values with a probability μ , independent of the identity of the letter and the other letters in the sequence, then the *probability* to mutate a sequence σ' to σ can be written as

$$p(\sigma' \rightarrow \sigma) = \left(\frac{\mu}{(\ell - 1)(1 - \mu)} \right)^{d(\sigma, \sigma')} (1 - \mu)^N. \quad (3)$$

Obviously, this probability is the same for all α_d sequences which are at a constant Hamming distance d from sequence σ , where α_d is given by

$$\alpha_d = \binom{N}{d} (\ell - 1)^d. \quad (4)$$

This can be seen by noting that there are $\binom{N}{d}$ ways of choosing d letters at which a sequence differs from σ and each of these d letters can take $\ell - 1$ values. For large N , most of the sequences are located in a belt of width $\sim \sqrt{N}$ around the distance $d_{\max} = N(\ell - 1)/\ell$ away from σ . Using (4), it is easily checked that $\sum_{\sigma} p(\sigma' \rightarrow \sigma) = 1$.

Similar to the transition from Wrightian to Malthusian fitness, in the continuous time limit the mutation probability (3) has to be replaced by the

mutation rate $\gamma(\sigma' \rightarrow \sigma)$, such that for generation time $\Delta t \rightarrow 0$

$$p(\sigma' \rightarrow \sigma) \approx \delta_{\sigma', \sigma} + \Delta t \gamma(\sigma' \rightarrow \sigma). \quad (5)$$

Denoting the mutation rate per letter by $\tilde{\mu}$ and setting $\mu = \tilde{\mu} \Delta t$ in (3) yields

$$\gamma(\sigma' \rightarrow \sigma) = \begin{cases} 0 & : d(\sigma', \sigma) > 1 \\ \tilde{\mu}/(\ell - 1) & : d(\sigma', \sigma) = 1 \\ -N\tilde{\mu} & : d(\sigma', \sigma) = 0 \end{cases}. \quad (6)$$

The normalization condition for mutation rates reads $\sum_{\sigma} \gamma(\sigma' \rightarrow \sigma) = 0$.

2.2 Mutation-selection models

We now discuss models of adaptation that incorporate the two competing processes discussed above, namely, mutation and selection. While mutation increases genetic diversity, selection tends to contain the population at fit sequences. In case selection wins out, one obtains a population in which individuals are genetically closely related else a heterogeneous population distributed over the entire sequence space results. In this article, we will mainly discuss the so-called *coupled models* in which the mutations occur only during replication. In the *paramuse models*, on the other hand, mutation and selection occurs in parallel, and they will be discussed here briefly. We refer the reader for more details to the reviews [10, 11] and references therein. While one may expect both types of mutation mechanisms to be relevant in describing evolution, the jury is still out on their relative importance. For this reason, both classes of models have been analysed in detail and the relationship between them has been explored, with regard to both static [23] and dynamic [24] properties.

The models discussed below work under the following two assumptions:

- (i) **Infinite population**, i.e., the total population size $M \gg \ell^N$, the total number of genotypes available. Under this assumption a deterministic description suffices and we can write down the time evolution equation for the average population fraction $X(\sigma, t)$ of sequence σ at time t . Although this is often unrealistic, the analysis is simpler in this limit which in many cases can be adapted to the finite population case to provide quantitative agreement with experiments [25, 26, 27]. The infinite population limit can be justified if the population is known to be localized in a small region of sequence space around a fitness peak, if one is interested in a short piece of the genome such as a single regulatory binding site [16] (see also Sect. 3.4) or if one works in the population genetics setting, where the letters in the sequence are alleles of a gene, rather than single nucleotides.
- (ii) **Asexual reproduction** which dominates in the lower forms of life such as virus and bacteria, and digital organisms. We will mainly consider haploid organisms but diploids are briefly discussed in Section 3.5. However, we do

not consider the case of sexual reproduction; a comparison between sexual and asexual reproduction modes in the context of sequence space models can be found in [28].

Paramuse models

In the paramuse models, introduced by Crow and Kimura [6], one assumes error-free replication and mutations are induced by the environment through radiation, thermal fluctuations etc. [10]. The equation for the rate of change $\dot{X}(\sigma, t) = \partial X(\sigma, t)/\partial t$ of the fraction $X(\sigma, t)$ of the population with sequence σ is given by

$$\dot{X}(\sigma, t) = [w(\sigma) - \sum_{\sigma'} w(\sigma') X(\sigma', t)] X(\sigma, t) + \sum_{\sigma'} \gamma(\sigma' \rightarrow \sigma) X(\sigma', t). \quad (7)$$

The first term is the selection term while the contribution from the mutations is contained in the last term. The evolution equation (7) is nonlinear in $X(\sigma, t)$ due to the second term on the right hand side, which is required to ensure the normalisation $\sum_{\sigma} X(\sigma, t) = 1$. This nonlinearity can be eliminated by passing to unnormalised population variables $Z(\sigma, t)$ defined by

$$Z(\sigma, t) = X(\sigma, t) \exp \left[\sum_{\sigma'} w(\sigma') \int_0^t d\tau X(\sigma', \tau) \right] \quad (8)$$

which satisfy the linear equation [29]

$$\frac{\partial Z(\sigma, t)}{\partial t} = w(\sigma) Z(\sigma, t) + \sum_{\sigma'} \gamma(\sigma' \rightarrow \sigma) Z(\sigma', t). \quad (9)$$

Equation (7) follows from (9) using the relation

$$X(\sigma, t) = \frac{Z(\sigma, t)}{\sum_{\sigma'} Z(\sigma', t)}. \quad (10)$$

Inserting the explicit form (6) for the mutation rates, it can be shown that the vector $\mathbf{Z}(t) = (Z(\sigma^1, t), \dots, Z(\sigma^S, t))$, where the index labels the $S = \ell^N$ points in sequence space, obeys a Schrödinger equation in imaginary time

$$\frac{\partial \mathbf{Z}(t)}{\partial t} = H \mathbf{Z}(t) \quad (11)$$

with quantum spin Hamiltonian H in one dimension. Specifically, for $\ell = 2$, one obtains the Hamiltonian of an Ising chain in the presence of a transverse magnetic field (mutations) with general interactions (specified by the fitness landscape) [29]; for an explicit example see Eq. (40). This model has been solved exactly for a variety of fitness landscapes using methods of quantum statistical physics [24, 29, 30]. A similar analysis has also been carried out for the biologically relevant case of $\ell = 4$ [31].

Coupled (quasispecies) dynamics

In the quasispecies model introduced by Eigen in the context of prebiotic evolution [4, 32, 33], the mutations are copying errors that occur during the reproduction process. This implies that the population fraction $X(\sigma, t)$ evolves according to

$$\dot{X}(\sigma, t) = \sum_{\sigma'} p(\sigma' \rightarrow \sigma) W(\sigma') X(\sigma', t) - \left(\sum_{\sigma'} W(\sigma') X(\sigma', t) \right) X(\sigma, t) \quad (12)$$

which can be linearised by a transformation analogous to (8) to yield the linear equation

$$\dot{Z}(\sigma, t) = \sum_{\sigma'} p(\sigma' \rightarrow \sigma) W(\sigma') Z(\sigma', t). \quad (13)$$

In discrete time this model takes the form

$$X(\sigma, t+1) = \frac{\sum_{\sigma'} W(\sigma') p(\sigma' \rightarrow \sigma) X(\sigma', t)}{\sum_{\sigma'} W(\sigma') X(\sigma', t)} \quad (14)$$

where the denominator arises due to the normalisation. The discrete time analog of the transformation (8) is given by

$$Z(\sigma, t) = X(\sigma, t) \prod_{\tau=0}^{t-1} \sum_{\sigma'} W(\sigma') X(\sigma', \tau) \quad (15)$$

As before, the unnormalised variables obey a linear equation given by

$$Z(\sigma, t+1) = \sum_{\sigma'} p(\sigma' \rightarrow \sigma) W(\sigma') Z(\sigma', t). \quad (16)$$

The use of the Wrightian (discrete time) fitness $W(\sigma)$ in the continuous time equation (12) requires some explanation. First, it ensures that the stationary solutions of (12) and (14) are identical. Second, it reflects the fact that (12) is invariant (up to a rescaling of time) under multiplication of the fitnesses by a constant factor, $W(\sigma) \rightarrow CW(\sigma)$, which is an exact symmetry of the discrete time equation (14), whereas the continuous time paramuse dynamics (7) is invariant under additive shifts $w(\sigma) \rightarrow w(\sigma) + C$ [10, 23]. In fact, (12) is *not* the continuous time limit of (14). Instead, inserting (1) and (5) in (14) and taking $\Delta t \rightarrow 0$, one obtains the paramuse dynamics (7). In this sense (12) is somewhat intermediate between the discrete time model (14) and the continuous time dynamics (7).

For the discrete time model (14) one can represent the evolutionary histories as configurations on a two-dimensional lattice with the two axes directed along the sequence and along time, with a spin variable $\sigma_i(t)$ at each site. Writing the evolution equation (16) for the vector $\mathbf{Z}(t)$ in the form

$$\mathbf{Z}(t+1) = T_{t+1,t} \mathbf{Z}(t) \quad (17)$$

then suggests to interpret $T_{t+1,t}$ as the transfer matrix of a two-dimensional classical spin model which relates the probability of a configuration in one row of the lattice to the next one [34]. For $\ell = 2$, this $2^N \times 2^N$ matrix can be written (up to a multiplicative constant) as

$$T_{t+1,t}[\{\sigma_i(t+1)\}, \{\sigma_i(t)\}] = \exp[\ln W(\{\sigma_i(t)\}) + J \sum_{i=1}^N \sigma_i(t+1)\sigma_i(t)] \quad (18)$$

where

$$J = \frac{1}{2} \ln(\mu^{-1} - 1). \quad (19)$$

Thus $T_{t+1,t} = \exp[-\tilde{H}]$, where \tilde{H} is the Hamiltonian of a two-dimensional Ising model² with nearest neighbor interactions of strength J along the time direction and general interactions [determined by the fitness landscape $W(\sigma)$] along the sequence direction [35]. The expression (19) shows that the interactions along the time direction are ferromagnetic (antiferromagnetic) whenever $\mu < 1/2$ ($\mu > 1/2$), while for $\mu = 1/2$ the sequence is completely randomized in each time step and the interaction vanishes.

Clearly, to obtain the distribution of sequences at time slice t , one needs to solve iteratively for all the $t - 1$ preceding layers. In the steady state for which $t \rightarrow \infty$ one requires the properties of the last “surface” layer coupled to a semi-infinite “bulk”. Since the transfer matrix (18) does not contain any couplings along the sequence direction in the last layer $t + 1$, the boundary condition for this semi-infinite spin model corresponds to a free surface [36].

3 Simple fitness landscapes

So far we have discussed the general equations governing the evolution of a population with mutations, but the fitness landscape was not specified. We do so now and begin with landscapes that are “simple” in that the fitness depends only on the distance from a given (*master*) sequence, which is usually the genotype of highest fitness³. Such landscapes are called *permutation invariant*, because the fitness depends only on the number of mismatches relative to the master sequence, but not on their position. Using this symmetry, the ℓ^N population variables can be grouped into $N + 1$ *error classes*, which greatly facilitates both numerical and analytic work [37].

3.1 The error threshold: Preliminary considerations

Much of this section is devoted to a discussion of the error threshold phenomenon, which refers to the loss of genetic integrity when mutations are

² The Ising Hamiltonian \tilde{H} should not be confused with the Hamiltonian H of the quantum spin chain in (11).

³ In the context of population genetics, the master genotype is often referred to as the *wild type*.

increased beyond a certain threshold. We consider only the stationary population distribution which is established after a long time. The linearity of both the continuous and discrete time evolution equations (9, 14, 16) implies that the stationary distribution is identical to the *principal eigenvector* of the matrix multiplying the population vector on the right hand side, i.e., the eigenvector with the largest eigenvalue. The principal eigenvalue is related to the mean population fitness in the stationary state. In this sense, the analysis of different fitness landscapes and mutation schemes is reduced to the investigation of the spectral properties of the corresponding evolution matrices [38].

The error threshold separates two regimes of mutation-selection balance characterized by a qualitatively different structure of the principal eigenvector. For small mutation rates the eigenvector is localized around the master sequence, i.e. only the entries corresponding to the dominant genotype and a few of its nearby mutants carry appreciable weight. Following Eigen and Schuster [32], such a localized population distribution is referred to as a *quasispecies*. When the mutation rate is increased beyond the error threshold, the principal eigenvector becomes delocalized and the population spreads uniformly throughout the sequence space. In this regime finite population effects, which are neglected in the models considered here, become extremely important: Rather than covering the entire sequence space, which is impossible given the vast number of sequences, a finite population forms a localized cloud which wanders about randomly [39].

Since the eigenvectors and eigenvalues of any finite matrix depend smoothly on its entries, the error threshold can become *sharp*, in the sense of being associated with some non-analytic behavior of the population distribution or the mean population fitness, only in the limit $N \rightarrow \infty$. We shall see below that in order to maintain the localized quasispecies in this limit, it is usually necessary to either reduce the single site mutation probability μ , such that the mutation probability per genome μN remains constant, or to increase the selective advantage of the master sequence with increasing N .

3.2 Error threshold in the sharp peak landscape

We demonstrate the error threshold in the case of a single sharp peak landscape which is defined as

$$W(\sigma) = W_0 \delta_{\sigma, \sigma_0} + (1 - \delta_{\sigma, \sigma_0}), \quad W_0 > 1. \quad (20)$$

Here σ_0 denotes the master sequence, and W_0 is the selective advantage of the master sequence relative to the other sequences, whose Wrightian fitness has been normalized to unity. We anticipate the error threshold to occur for $\mu \rightarrow 0$, $N \rightarrow \infty$, keeping the mutation rate per genome μN finite. Let us consider the coupled model in discrete time⁴ defined by (14) with the choice

⁴ Recall that in the steady state, both versions of the coupled model are identical.

(20). In the limit $\mu \rightarrow 0$ the mutations taking the mutants back into the master sequence can be neglected⁵, and the only nonzero contribution to $X(\sigma_0)$ on the right hand side of (14) is that for $\sigma' = \sigma$. This yields

$$X(\sigma_0) = \frac{W_0 e^{-\mu N} - 1}{W_0 - 1} \quad (21)$$

which is an acceptable solution provided $\mu N \leq \ln W_0$. Thus, a phase transition occurs at the critical mutation probability

$$\mu_c = \frac{\ln W_0}{N} \quad (22)$$

beyond which the population cannot be maintained at the peak of the landscape. Close to μ_c , the fraction of population at the master sequence behaves as

$$X(\sigma_0) \approx \frac{N}{W_0 - 1} (\mu_c - \mu) \quad (23)$$

thus approaching zero continuously at μ_c . The above results are also confirmed by a detailed numerical analysis for finite μ and N , in which the population was grouped into error classes at constant Hamming distance from the master sequence and the population in the error classes as well as the eigenvalues of the evolution matrix were followed as a function of μ [37].

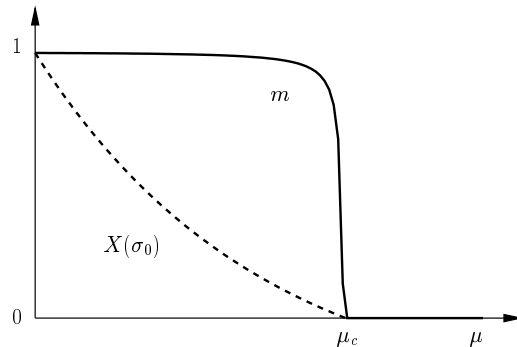


Fig. 2. Figure to show the continuous transition in the fraction $X(\sigma_0)$ of the master sequence and the (almost) discontinuous one in the overlap m as a function of mutation rate μ , for $N = 1000$ and $W_0 = 4$.

⁵ Neglecting back mutations towards the master sequence is common in population genetics, where it is referred to as a *unidirectional* mutation scheme [11]. It simplifies the analytic treatment [28, 40], and will be used repeatedly in this article as an approximation which is expected to become exact for $\mu \rightarrow 0$, $N \rightarrow \infty$.

The way in which the error threshold condition (22) combines mutation rate, sequence length and selective advantage is the central result of quasispecies theory. In particular, it shows that in order to maintain a localized quasispecies at finite single site mutation rate in the limit $N \rightarrow \infty$, the selective advantage has to increase *exponentially* with N [41]. Under the assumption that typical selective advantages do not depend strongly on sequence length, Eq. (22) also provides some rationalization for the observation that the product μN is roughly constant within classes of similar organisms (see Sect. 2.1). On the other hand, at given achievable values of the replication accuracy and the selective advantage, the condition $\mu < \mu_c$ place an upper bound N_{\max} on the sequence length, beyond which genetic integrity is lost. Elsewhere in this book Ester Lázaro presents substantial evidence that RNA viruses have evolved to reside close to this threshold, possibly because this allows them to maintain a maximal genetic variability which is needed to rapidly adapt to changing environments (see also Sect. 6.2).

Neglecting back mutations to the master sequence allows to derive an expression for the mean Hamming distance to the master sequence, which reads [40]

$$\langle d(\sigma, \sigma_0) \rangle = \frac{W_0 N \mu}{W_0 e^{-N\mu} - 1}. \quad (24)$$

The mean Hamming distance is finite for $\mu < \mu_c$ and diverges as $(\mu_c - \mu)^{-1}$ as the error threshold is approached. This provides an alternative characterisation of the threshold. A related quantity, which has been proposed as an order parameter for the transition, is the *mean overlap*

$$m = 1 - \frac{2\langle d(\sigma, \sigma_0) \rangle}{N} \quad (25)$$

between the master sequence and a randomly chosen sequence [41]. Since $\langle d(\sigma, \sigma_0) \rangle$ remains finite for $N \rightarrow \infty$ in the localised phase, the overlap is $m = 1$ in this limit and jumps discontinuously to $m = 0$ at the threshold. Figure 2 displaying the two order parameters considered in the above discussion illustrates that the nature of the transition – continuous or discontinuous – depends to some extent on the quantity under consideration⁶.

Yet another characterization of the error threshold relies on the notion of the *consensus sequence* σ^c , which carries at each site i that letter σ_i^c which is most frequently represented in the population. It is easy to see that, for symmetry reasons, the consensus sequence in the sharp peak landscape (20) coincides with the master sequence, $\sigma^c = \sigma_0$, throughout the localized phase; this is true for general permutation-invariant single peak landscapes. In the

⁶ In contradiction to the discussion above, a numerical study based on the mapping to a two-dimensional Ising model described in Sect. 2.2 deduced that both m and $X(\sigma_0)$ change smoothly at the transition [36]. However in this study, a scaling analysis with genome length (akin to finite size scaling analysis in statistical mechanics) was not carried out to obtain the behavior in the limit $N \rightarrow \infty$.

delocalized phase, where the population is uniformly spread throughout sequence space for $N \rightarrow \infty$, all letters appear with equal probability and the consensus sequence cannot be defined. This is an artifact of the assumption of infinite population size: a finite population retains some genetic structure even in a flat fitness landscape and diffuses through sequence space as a cloud centered around a moving consensus sequence $\sigma^c(t)$ [39]. Thus at the error threshold the consensus sequence ceases to be pinned to the master sequence and becomes time-dependent. This criterion to locate the transition is particularly useful in complex fitness landscapes, where the most-fit master sequence is not known [42] (see Sect.4). Similarly, in experimental studies of microbial populations such as RNA viruses, the consensus sequence is taken to represent the (unknown) wildtype genome, and the genetic spread of the population around σ^c is interpreted as a measure of the balance between mutational and selective forces (see the chapter by E. Lázaro).

3.3 Exact solution of a sharp peak model

A variant of Eigen's model was solved exactly for any N in [43]. The model is defined in discrete time but the mutations are restricted to mutants within Hamming distance equal to one, as for the continuous time mutation rates (6). In addition, mutations are assumed to occur in the whole population *before* the reproduction process. With the fitness landscape (20) this leads to the linear evolution equation

$$Z(\sigma, t + 1) = [1 + (W_0 - 1)\delta_{\sigma, \sigma_0}] \times \quad (26)$$

$$\times \left[(1 - N\mu)Z(\sigma, t) + \mu \sum_{\sigma'} Z(\sigma', t) \delta_{d(\sigma', \sigma), 1} \right]$$

for the unnormalised population variables. Note that the model is well defined only for $N\mu < 1$.

At large times, $Z(\sigma, t + 1) \approx \Lambda Z(\sigma, t)$ where Λ is the largest eigenvalue of the evolution matrix on the right hand side of (27). In the delocalised phase, the population is spread over the entire sequence space with mean fitness $W = 1$, so that $\Lambda = 1$ whereas in the localised phase, a finite fraction has fitness $W_0 > 1$ and hence $\Lambda > 1$. For any N , the eigenvalue Λ is determined by the exact equation

$$\frac{W_0}{W_0 - 1} = \frac{1}{2^N} \sum_{k=0}^N \binom{N}{k} \frac{\Lambda}{\Lambda - 1 + 2k\mu}. \quad (27)$$

Due to the $k = 0$ term on the RHS of the above equation, it is evident that Λ can take a value equal to 1 only in the $N \rightarrow \infty$ limit. Thus, there is no phase transition for any finite N .

In the limit $N \rightarrow \infty$, $\mu \rightarrow 0$ with $N\mu < 1$ fixed the eigenvalue is given by the expression

$$\Lambda = \max\{1, W_0(1 - N\mu)\}, \quad (28)$$

which sticks to unity beyond the critical mutation strength

$$\mu_c = \frac{W_0 - 1}{W_0 N}. \quad (29)$$

Incidentally, the above expression for μ_c can be obtained using (21) by expanding the exponential to first order in μN . This is required to ensure that $\mu N < 1$ is satisfied for any $W_0 > 1$. In both cases the selective advantage needed to localize the quasispecies is the inverse of the *copying fidelity*, i.e. the probability of creating an error-free offspring.

The behavior of other quantities at the threshold follow from that of Λ . For example, the fraction of the population residing at the master sequence is given by

$$X(\sigma_0) = \frac{W_0(\Lambda - 1)}{(W_0 - 1)\Lambda} \quad (30)$$

which vanishes linearly in $\mu_c - \mu$ at the threshold, and the mean Hamming distance from the master sequence is

$$\langle d(\sigma, \sigma_0) \rangle = \frac{N\mu}{\Lambda - 1} \quad (31)$$

which diverges as $(\mu_c - \mu)^{-1}$. The expressions (29 - 31) are valid in the asymptotic limit $N \rightarrow \infty$, but systematic expansions of these quantities in powers of $1/N$ are also available [43].

Comparing the expressions (23) and (24) to (30) and (31) respectively, we see that $X(\sigma_0)$ and $\langle d(\sigma, \sigma_0) \rangle$ behave qualitatively similar in the two models as the error threshold is approached. This is a simple example of the principle of *universality* commonly encountered at physical phase transitions, which states that the way in which singular quantities vanish or diverge at the transition is independent of detailed properties of the model.

3.4 Modifying the shape of the fitness peak

Since the sharp peak landscape (20) was chosen for its simplicity, and not because it is expected to be biologically realistic, it is important to investigate how the error threshold phenomenology depends on the shape of the fitness peak. In this section we discuss some illustrative examples. A method for solving the stationary quasispecies equation for general peak shapes has been developed by Peliti [44]. It employs a strong selection limit, in which the fitness is written as $W(\sigma) = \exp[N\Phi(\sigma)]$ and the limit $N \rightarrow \infty$ is carried out at fixed mutation probability μ .

Peak height versus peak width

We first consider a landscape with one sharp global maximum and a broad peak of lower fitness separated by a flat landscape. This is defined as

$$W(\sigma) = W_0\delta_{\sigma,\sigma_0} + W_N\delta_{\sigma,\sigma^N} + W_{N-1}\delta_{d(\sigma,\sigma^N),1} + \sum_{j \neq 0, N-1, N} \delta_{d(\sigma,\sigma_0),j} \quad (32)$$

where σ^N is the sequence at maximal Hamming distance N from σ_0 and $W_0 > W_N > W_{N-1} > 1$. By placing the two fitness peaks at the two poles σ_0 and σ^N of the sequence space, the permutation symmetry of the landscape is preserved and the population can be subdivided into error classes. The coupled model with the landscape (32) has been studied in both continuous [45] and discrete time [36]. Interestingly, with increasing mutation rate, the quasispecies shifts abruptly from the sequence σ_0 to the broader peak around σ^N finally delocalising over the whole sequence space. For large mutation rates, the quasispecies is more comfortable at the lower peak surrounded by an extended region of elevated fitness than at the (globally optimal) isolated master sequence.

Mesa landscapes

Broad fitness peaks arise naturally in the evolution of regulatory binding sites [16, 46, 47]. In this context the fitness of a given regulatory sequence can be plausibly related to the binding probability of the corresponding transcription factor. Simple thermodynamic models predict that the binding probability depends on the number of mismatches $d(\sigma, \sigma_0)$ with respect to the regulatory master sequence σ_0 through a Fermi function,

$$p_b(d) = \frac{1}{1 + \exp[\epsilon(d - d_0)/k_B T]}, \quad (33)$$

where ϵ is the binding energy per mismatch, ϵd_0 is the chemical potential corresponding to the concentration of the transcription factor, and $k_B T$ is the thermal energy at temperature T . For $\epsilon/k_B T \gg 1$ the binding probability drops abruptly from $p_b = 1$ to $p_b = 0$ when d exceeds the number d_0 of tolerable mismatches; a typical value of this ratio is $\epsilon/k_B T \approx 2$.

In the simplest scenario, the selective advantage of a regulatory sequence is assumed to be proportional to the binding probability. This leads to a *mesa-shaped* fitness landscape, with a plateau of constant fitness and radius d_0 around the master sequence. In [16] a detailed study of the error threshold in this landscape was presented for continuous time paramuse dynamics with fitness landscape $w(d) = w_0 p_b(d)$. An exact solution is possible in a limit where d becomes a continuous variable and the Fermi function (33) is replaced by a step function. Provided $d_0 \ll N$, the error threshold is found to take place at a critical mutation strength μ_c given by

$$\mu_c = \frac{2w_0}{N(1 + \eta^2/d_0^2)}, \quad (34)$$

where η is a constant of order unity. The critical mutation strength is seen to increase with increasing d_0 , illustrating the enhanced stability of the quasispecies with increasing width of the fitness peak. In the localized phase, the majority of the population is located near the mesa edge at $d = d_0$, reflecting the exponential increase of the number (4) of available genotypes with distance d . This is a purely entropic effect, which leads to a maximal *fuzziness* of regulatory motifs.

Somewhat more realistically, one expects that the fitness depends not only on the ability of the sequence to bind the transcription factor in a certain cellular state, but also on its ability to *avoid* binding in other states. This can be modeled by a fitness function which is proportional to the difference between two Fermi functions (33) with different values of d_0 , leading to a *crater* landscape with a rim of high fitness around a fitness minimum at $d = 0$ [47].

Epistasis: Coupled dynamics

Not all landscapes display the error threshold phenomenon. We illustrate this point using the multiplicative (or Fujiyama) landscape as an example. In this case

$$W(\sigma) = \prod_{i=1}^N e^{\lambda\sigma_i} = \exp[\lambda(N - 2d(\sigma_0, \sigma))], \quad (35)$$

where for simplicity we choose $\ell = 2$ and let σ_i take values ± 1 . For $\lambda > 0$ the master sequence is $\sigma_0 = (1, 1, 1, \dots, 1)$ and the Hamiltonian \tilde{H} obtained from (18) is

$$\tilde{H} = \sum_{i=1}^N [-J\sigma_i(t+1)\sigma_i(t) - \lambda\sigma_i(t)]. \quad (36)$$

Due to the absence of interactions along the sequence space direction, one obtains, for each position i , a one-dimensional Ising model in the presence of magnetic field λ . This model is well known to lack a phase transition and due to the λ term, the spins tend to align in the direction of the field. Correspondingly, a finite fraction of the population is maintained at the master sequence for any value of the mutation rate. The full population distribution has been worked out in [48].

In genetic terms, the multiplicative form (35) implies that the different gene loci contribute independently to the fitness, which is referred to as the absence of *epistatic interactions*. In general, one must distinguish between *synergistic* or *negative* epistasis, in which the (deleterious) effect of an additional mutation *increases* with increasing distance from the wild type (master sequence), and *diminishing returns* or *positive* epistasis, when the effects of

mutations decreases with increasing distance⁷. The sharp peak landscape (20) is an extreme case of positive epistasis, because after the first mutation away from the master sequence, any additional mutation does not affect the fitness at all. An extreme limit of negative epistasis is represented by the case of truncation selection, where the Wrightian fitness vanishes beyond a critical Hamming distance d_c [49]. As we discuss below, whether or not an error threshold occurs depends on the behavior of the landscape at large Hamming distance from the master sequence.

Consider a general fitness landscape defined by [40]

$$W(\sigma) = q(1-s)^{d(\sigma, \sigma_0)^\alpha} + 1 - q \quad (37)$$

where $0 \leq q, s \leq 1$ and $\alpha > 0$. Two cases need to be distinguished: for $q < 1$, the lower bound on the fitness is nonzero and when $s \rightarrow 1$ it becomes of sharp peak type (20) with the (relative) selective advantage $1/(1-q)$ for the master sequence, while for $q = 1$, the multiplicative form (35) with $\lambda = -\ln(1-s)$ is recovered for $\alpha = 1$, and $\alpha > 1$ ($\alpha < 1$) describes a situation with negative (positive) epistasis (Fig. 3).

The error threshold can be computed in the unidirectional approximation (no back mutations towards the master sequence), and in the limit $N \rightarrow \infty$, $\mu \rightarrow 0$, for $\alpha = 1, q < 1$, it has been shown that the critical mutation strength $\mu_c = N^{-1} \ln[1/(1-q)]$, which is of exactly the same form as the sharp peak result (22). For $q = 1$, a similar analysis shows that (37) displays an error threshold only when $\alpha < 1$, with a critical mutation strength given by $\mu_c = N^{\alpha-1} \lambda$ [40]. Note that in this case, the correct scaling is obtained in the limit $N \rightarrow \infty, \mu \rightarrow 0$ keeping $\mu N^{1-\alpha}$ fixed.

The above results can be understood using the following result for general *bounded* Wrightian fitness landscapes with $0 < W_{\min} \leq W(\sigma) \leq W_{\max} < \infty$. For such landscapes, the master sequence is lost from the population at a critical mutation probability which satisfies (in the unidirectional approximation and for $N \rightarrow \infty$) [40]

$$\mu_c \leq \frac{1}{N} \ln(W_{\max}/W_{\min}); \quad (38)$$

a similar result is proved in [50]. If the right hand side of (38) diverges as $N \rightarrow \infty$, this would imply that there is no finite error threshold and the master sequence is maintained at any mutation rate while its vanishing would be consistent with the existence of a sharp transition for $\mu \rightarrow 0, N \rightarrow \infty$. For $q = 1$, the ratio between the largest and the smallest fitness is $W_{\max}/W_{\min} = e^{\lambda N^\alpha}$, so that the right hand side of (38) vanishes for $N \rightarrow \infty$ only when $\alpha < 1$ whereas it goes to zero for any $\alpha > 0$ for $q < 1$, in agreement with the results cited above. The case of the multiplicative landscape (35) is special; here $W_{\max}/W_{\min} = e^{2\lambda N}$ and (38) would suggest a finite error threshold⁸. However,

⁷ This nomenclature is based on [11, 40], but it does not appear to be unambiguous; in [49] a definition of positive and negative epistasis is used which is opposite to the present one.

⁸ The unidirectional approximation erroneously predicts a transition at $\mu_c = s$ [40].

as discussed earlier, the master sequence is maintained at any mutation rate for $\alpha = q = 1$.

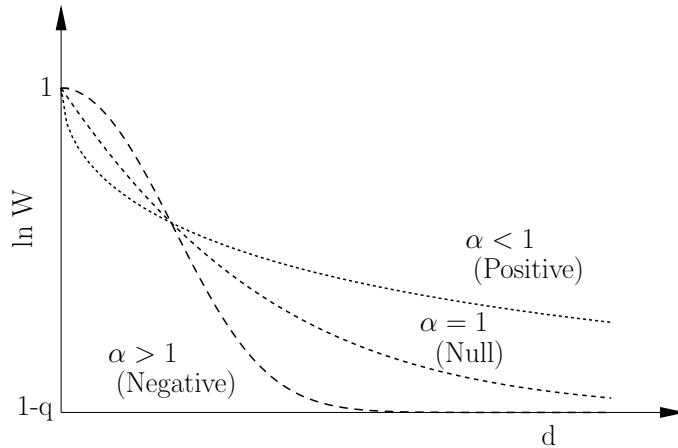


Fig. 3. Illustration of the fitness landscape (37) with $s = q = 0.5$ and three different values of α .

The general conclusion from these considerations is that the existence of an error threshold requires positive epistasis. This can be understood from the following qualitative argument [40]: For the case of positive epistasis, the selection force towards the fitness peak that has to be overcome by mutations is largest close to the peak; once this initial barrier has been surpassed, the population delocalises completely. In contrast, for negative epistasis, each additional step away from the fitness peak requires a larger mutation pressure than the previous step, and hence the population remains localised.

Epistasis: Paramuse models

Since Malthusian fitness is essentially the logarithm of Wrightian fitness, the absence of epistatic interactions in continuous time models implies a *linear* dependence of the fitness $w(\sigma)$ on $d(\sigma, \sigma_0)$. To investigate the effects of epistasis, a quadratic fitness landscape of the form

$$w(\sigma) = a[1 - 2d(\sigma, \sigma_0)/N] + \frac{1}{2}b[1 - 2d(\sigma, \sigma_0)/N]^2 \quad (39)$$

has been considered [11], with $a > 0$ and $b > 0$ ($b < 0$) for positive (negative) epistasis. This choice of parameters leads, through the mapping described in Sect. 2.2, to the quantum spin Hamiltonian

$$H = \tilde{\mu} \sum_{i=1}^N (\sigma_i^x - 1) + a \sum_{i=1}^N \sigma_i^z + \frac{b}{2N} \sum_{ij} \sigma_i^z \sigma_j^z, \quad (40)$$

where σ_i^x and σ_i^z denote the x - and z -components of the quantum mechanical spin operator. As in the discrete time case, in the absence of epistasis ($b = 0$) the spins at different sites i are independent. Epistasis introduces a coupling between any pair i, j of spins, independent of their position in the sequence. In the language of statistical mechanics, this is an interaction of *mean field* type; it is ferromagnetic for $b < 0$ and antiferromagnetic for $b > 0$.

An explicit solution of the model has been presented for the case $a = 0$, $b > 0$ [11]. In the limit $N \rightarrow \infty$, the mean overlap (25) is given by the expression

$$m = \max[1 - \tilde{\mu}/b, 0], \quad (41)$$

which, in contrast to the case of the sharp peak landscape, vanishes *continuously* at $\tilde{\mu} = b$. In general, an error threshold exists only if $-b \leq a < 0$. This implies that the fitness displays a minimum at a distance $0 < d_{\min} \leq N/2$ from the master sequence.

3.5 Beyond the standard model

In this section we discuss a few biologically motivated generalisations of the mutation-selection models described so far, while however maintaining the basic simplicity of the fitness landscape.

Diploid models

The evolution equations for diploid organisms are similar to those for the haploid case, except that the fitness $W(\sigma)$ is replaced by the marginal fitness

$$\tilde{W}(\sigma, t) = \sum_{\sigma'} W(\sigma, \sigma') X(\sigma', t), \quad (42)$$

where $W(\sigma, \sigma')$ is the fitness of an individual with diploid genotype (σ, σ') , and $X(\sigma, t)$ is the fraction of individuals carrying sequence σ in either one of their two sets of genes [23, 51]. The analog of the sharp peak landscape (20) is given by

$$W(\sigma, \sigma') = \begin{cases} W_0 & : \sigma = \sigma' = \sigma_0 \\ W_1 & : \text{either } \sigma = \sigma_0 \text{ or } \sigma' = \sigma_0 \\ W_2 & : \text{both } \sigma, \sigma' \neq \sigma_0 \end{cases} \quad (43)$$

with $W_0 \geq W_1 \geq W_2$. In the absence of dominance effects ($W_1 = \sqrt{W_0 W_2}$ for Wrightian fitness or $w_1 = (w_0 + w_2)/2$ for Malthusian fitness) the problem

can be reduced to the haploid case. However, in general, a transformation to a linear equation, as described in Sect. 2.2, is unknown for the diploid case; the equations are inherently nonlinear because of the dependence of the marginal fitness (42) on the population distribution. As a consequence, there are multiple solutions for the fraction $X(\sigma_0)$ of wild type individuals. Nevertheless, error threshold phenomena occur whose locations depend on the relative values of W_0 , W_1 and W_2 . For instance, the critical mutation rate is roughly doubled as compared to the haploid model in the case of complete dominance of the wild type ($W_0 = W_1 > W_2$).

Semiconservative replication

While the quasispecies model described in Sect. 2.2 is appropriate for organisms with RNA as genetic material, it needs to be amended for DNA-based organisms. The genotype corresponding to a double stranded DNA molecule can be represented by $\{\sigma, \bar{\sigma}\}$ where $\bar{\sigma}$ is the complementary strand of σ . The replication process involves splitting the DNA and pairing each strand with the complementary bases to produce two daughter DNA's. Thus, only one strand of the original DNA is conserved in the daughter DNA. However, copying errors and subsequent (imperfect) repair result in a different DNA genotype $\{\sigma', \bar{\sigma}'\}$. Thus, the (unnormalised) number of individuals of genotype $\{\sigma, \bar{\sigma}\}$ evolves in time as [52]

$$\begin{aligned} \dot{Z}(\{\sigma, \bar{\sigma}\}, t) &= -W(\{\sigma, \bar{\sigma}\})Z(\{\sigma, \bar{\sigma}\}, t) \\ &+ \sum_{\{\sigma', \bar{\sigma}'\}} (p(\sigma' \rightarrow \{\sigma, \bar{\sigma}\}) + p(\bar{\sigma}' \rightarrow \{\sigma, \bar{\sigma}\})) W(\{\sigma', \bar{\sigma}'\})Z(\{\sigma', \bar{\sigma}'\}, t) \end{aligned} \quad (44)$$

where $p(\sigma' \rightarrow \{\sigma, \bar{\sigma}\})$ is the probability that parent strand σ' produces $\{\sigma, \bar{\sigma}\}$ and the first term represents the loss of the original genome. For the sharp peak landscape, the error threshold occurs at

$$\mu_c = \frac{2}{N} \ln \left(\frac{2W_0}{1 + W_0} \right) \quad (45)$$

which saturates for $W_0 \rightarrow \infty$ unlike (22), so that the loss of the master sequence can not be avoided by increasing its selective advantage. This can be traced back to the destruction of the parent genome in the semiconservative case, which implies that, at sufficiently high mutation probability per genome, increasing the reproduction rate of the master sequence actually accelerates its extinction.

Dynamic landscapes

The assumption of a static fitness landscape is good when evolution occurs on short time scales or in long-term, controlled experiments in the laboratory.

However, natural populations are usually subjected to dynamic environments such as that of pathogens living in a host with a dynamic immune system. For the problem of formation of quasispecies in the presence of a dynamic sharp peak landscape, two cases need to be distinguished – one when the fitness W_0 of the master sequence σ_0 is fixed but its location shifts at periodic time intervals of length τ to a nearest neighbor [53], and the other in which the location is kept fixed but the height of the peak changes with time [54, 55].

In the former case, besides the usual upper limit on the mutation rate, an analytical approximation of the model shows the existence of a lower limit also [53]. The latter arises because when the peak shift occurs, at least one individual should be present at the new location so that it can replicate and form the quasispecies. For too low mutation rates, this may not happen and this effect is likely to be more pronounced for finite populations.

In the case of a time-dependent peak height $W_0(t)$ of the master sequence, the characteristic time scale τ of variation of the fitness landscape must be compared to the response time of the population, which is the inverse of the relative growth rate of the master sequence compared to its mutants. When τ is large compared to the response time the population fraction at the master sequence follows the landscape quasistatically. For rapidly changing landscapes the time-averaged population undergoes an error threshold transition at the mutation strength μ_c given by [54, 55]

$$(1 - \mu_c)^N = \left(\frac{\int_0^T W_0(t) dt}{T} \right)^{-1} \quad (46)$$

which generalises (22) by replacing the static fitness by an average over a time interval of length $T \gg \tau$. For periodic $W_0(t)$ with period τ the fraction $X(\sigma_0, t)$ also changes periodically with the same period but with a phase shift that increases with decreasing τ [55]. Due to this time lag, the master sequence achieves maximum population when its fitness has already dropped from the maximum amplitude.

Parental effects

Digital organisms are computer programs with a set of instructions (genome) including copy commands due to which they can be replicated. During the copying process, some instructions can get deleted, repeated or replaced. An evolved program can perform complex logic operations by using a simple logic operator available to it. Such complex organisms are selected by allotting them more CPU time thus increasing their replication rate defined as the ratio of the number of logical instructions that they can execute to the number of instructions that they have to perform in order to produce a new program [18]. While the latter depends on the individual's own genome, the CPU time available to it is a parental influence.

The situation is analogous to the case of biological organisms which obtain proteins etc. from the parent besides the genome. In such a case, the fraction $X(\sigma', \sigma, t)$ of population at sequence σ with ancestor σ' evolves as [56]

$$\dot{X}(\sigma', \sigma, t) = \sum_{\sigma''} A(\sigma'')W(\sigma')p(\sigma' \rightarrow \sigma)X(\sigma'', \sigma', t) - f(t)X(\sigma', \sigma, t) \quad (47)$$

where $f(t) = \sum_{\sigma'', \sigma'} A(\sigma'')W(\sigma')X(\sigma'', \sigma', t)$ and $A(\sigma')$ is the contribution to the fitness from the ancestor. In the absence of parental effects, $A(\sigma) = 1$ for all sequences and the original equation (12) is obtained for $X(\sigma, t) = \sum_{\sigma'} X(\sigma', \sigma, t)$. This can be generalised by weighting the population variable by the parental contribution and defining the normalised variable

$$X(\sigma, t) = \sum_{\sigma'} A(\sigma')X(\sigma', \sigma, t) / \sum_{\sigma', \sigma''} A(\sigma')X(\sigma', \sigma'', t) \quad (48)$$

which reduces the ℓ^{2N} variables in (47) to ℓ^N . Interestingly, in the steady state the population $X(\sigma, t)$ obeys the quasispecies equation (12) with fitness $A(\sigma)W(\sigma)$. Thus the available results for the standard quasispecies model can be directly applied to this case. In particular, for the sharp peak landscape the fraction $X(\sigma_0, \sigma_0)$ at the master sequence increases (relative to the null case when there are no parental effects) if the ancestral fitness $A(\sigma_0) > A(\sigma)$ for $\sigma \neq \sigma_0$. It is also possible to obtain the opposite trend if the ancestral effect is deleterious and has to be compensated by the fitness of the individual itself, such as when $A(\sigma_0) < A(\sigma)$ and $W(\sigma_0) > W(\sigma)$.

Heterogeneous mutations

The accuracy of replication depends on enzymes called polymerases which can be present in different types with their respective accuracies. For example, as discussed by E. Lázaro elsewhere in this book, RNA virus strains that show resistance to certain mutagens may possess polymerases with a particularly high copying fidelity. In the presence of p polymerases with concentrations c_k and replication error μ_k , $k = 1, \dots, p$, the mutation probability (3) generalises to

$$p(\sigma' \rightarrow \sigma) = \sum_{k=1}^p c_k \left(\frac{\mu_k}{(\ell-1)(1-\mu_k)} \right)^{d(\sigma, \sigma')} (1-\mu_k)^N. \quad (49)$$

One may expect that by increasing the concentration of the polymerase with low error rate, the error threshold can be increased (even to infinity). That this indeed is the case was demonstrated in [57] for $p = 2$ with concentration c of an error-free polymerase with replication error probability $\mu_1 = 0$ and $1-c$ of an error-prone polymerase with $\mu_2 = \mu > 0$. For the sharp peak landscape, one can find the fraction $X(\sigma_0) = W_0 p(\sigma_0 \rightarrow \sigma_0) / (W_0 - 1)$ of the master sequence by neglecting the back mutations as before where $p(\sigma_0 \rightarrow \sigma_0) \approx c + (1-c)e^{-\mu N}$

for $\mu \rightarrow 0$ and $N \rightarrow \infty$. Then the master sequence can localise the population if

$$\mu > \mu_c = \frac{1}{N} \ln \left(\frac{1-c}{W_0^{-1}-c} \right) \quad (50)$$

which reduces to (22) for $c = 0$ as expected and increases with increasing c . Since the argument of the logarithm should be positive for real μ , it follows that $c < c' = 1/W_0$ and on exceeding c' , the master sequence continues to localise population for any mutation rate.

4 Complex fitness landscapes

We now turn our attention to “complex” landscapes which do not possess the symmetries of the simple ones discussed in the last section. Realistic landscapes are expected to have hills, valleys, basins and ridges [19]. A pictorial representation of such a *rugged* fitness landscape drawn over a two-dimensional plane is shown in Fig. 4. Despite the intuitive appeal of such pictures, however, it should be kept in mind that they are metaphors rather than models of biological reality. Real fitness landscapes extend over the very high dimensional, discrete space of genotype sequences, and there are indications that the intuition gained in our experience with low-dimensional landscapes fails when applied to such abstract objects [2].

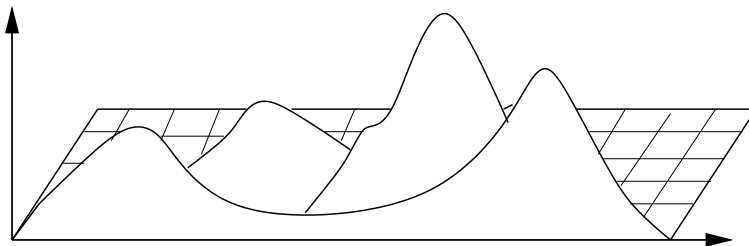


Fig. 4. Schematic representation of a rugged fitness landscape defined over a two-dimensional genotype space.

Researchers trying to construct realistic fitness landscapes have followed one of two basic approaches. One approach is to study simple model systems for which the mapping from genotype to phenotype can be carried out explicitly. This has been pursued in great detail for the case of RNA sequences, which will be briefly described in Sect. 4.1, as well as for proteins; for a detailed discussion we refer to the chapters by P. Schuster and P. Stadler, and by U. Bastolla, M. Porto, H. E. Roman and M. Vendruscolo in this book. The second approach, which was conceptually inspired by the statistical physics of disordered systems [58, 59], is to regard a given fitness landscape as the

realization of an *ensemble of random functions* with prescribed statistical properties. In this case an important quantity characterising the ruggedness of the landscape is the correlation coefficient $\rho(d, N)$ between the fitnesses of two genotypes at Hamming distance d , which is defined as

$$\rho(d, N) = \frac{\langle w(\sigma)w(\sigma') \rangle - \langle w(\sigma) \rangle^2}{\langle w(\sigma)^2 \rangle - \langle w(\sigma) \rangle^2}, \quad d = d(\sigma, \sigma'). \quad (51)$$

Here the angular brackets stand for an average over the ensemble of landscape configurations and the denominator ensures that $\rho(0, N)$ is scaled to unity. We have defined (51) in terms of Malthusian fitness, but the Wrightian case can be treated in the same way. Examples of random fitness landscapes will be discussed in Sections 4.2, 4.3 and 4.4.

4.1 An explicit genotype-phenotype map for RNA sequences

For the description of evolution experiments with self-replicating RNA molecules (see Sect. 6.1), it is natural to assume that the fitness of a given RNA sequence depends only on the three-dimensional shape that the molecule folds into in the solution. As an approximation to the full three-dimensional shape (the *ternary* structure of the molecule), its *secondary* structure, defined as the set of allowed base pairings that satisfies the no-knot constraint and minimises the free energy, can be used. In contrast to ternary structure, the secondary structure can be computed from the sequence by efficient algorithms. Although this does not yet solve the problem of how to assign a fitness to the genotype, it allows to study in great detail the mapping from the genotype (the sequence) to the phenotype (the secondary structure) [20, 60, 61].

The most important feature of this mapping is that it is *many-to-one*. Indeed, the number of secondary structures of random RNA sequences of length N behaves asymptotically as [61]

$$\mathcal{N}_{\text{RNA}} \approx 1.4848 \times N^{-3/2} \times (1.8488)^N, \quad (52)$$

whereas the number of sequences is 4^N . Thus exponentially many sequences fold into the same secondary structure for large N . Since sequences with the same secondary structure must be assigned the same fitness, it follows that the fitness landscape contains large regions of constant fitness, which are therefore selectively *neutral*. Typically there are a few common structures (which are represented by many sequences) and many more rare ones, with the distribution of the number of sequences mapping to a given structure following a power law. The most common structures form *neutral networks* extending throughout sequence space, such that any randomly chosen sequence is close to a sequence on this network. Similar networks have also been found in the sequence space of proteins [62, 63, 64], see the chapter by U. Bastolla, M. Porto, H.E. Roman and M. Vendruscolo in this book. Some aspects of the evolutionary process on such neutral networks will be discussed below in Sections 4.4 and 5.1.

4.2 Uncorrelated random landscapes

The simplest kind of random fitness landscape is the uncorrelated landscape where the fitnesses are independent random variables drawn from some common probability distribution [59]. In this case the correlation function (51) reduces to $\rho(d, N) = \delta_{d,0}$. An example from this class is the Random Energy Model (REM) of spin glass theory [65, 66, 67], for which the (Wrightian) fitness is given by

$$W(\sigma) = \exp[\kappa E(\sigma)], \quad (53)$$

where the “energies” E are independent Gaussian random variables with distribution

$$P(E) = \frac{1}{\sqrt{\pi N}} \exp(-E^2/N), \quad (54)$$

and κ is an “inverse selective temperature”.

This model displays a phase transition which is quite similar to the error threshold in the single peak landscape. At high mutation rates the population is delocalised while at low mutation rates it is frozen into the master sequence, which in this case is simply the sequence σ_{\max} with the largest value E_{\max} of $E(\sigma)$ in the particular realization (the “ground state” configuration of the REM). The scaling with N in (54) is chosen such that this maximal value is proportional to N , $E_{\max} = N\sqrt{\ln 2}$ to leading order. At the transition the mean overlap (25) jumps discontinuously from one to zero [41].

The critical mutation probability required for delocalisation can be computed along the lines used in Sect. 3.2 for the sharp peak landscape. Neglecting back mutations to σ_{\max} , a nonzero population fraction $X(\sigma_{\max})$ is maintained if the product of $W_{\max} = \exp[\kappa E_{\max}]$ with the probability $(1 - \mu)^N$ of producing an error-free offspring is greater than the mean population fitness \bar{W} in the delocalised phase [12]. The latter is obtained by averaging (53) with respect to the distribution (54), which yields $\bar{W} = \exp[\kappa^2 N/4]$. Comparing the two expressions, one finds [12, 41, 67]

$$\mu_c = 1 - \exp[\kappa^2/4 - \kappa\sqrt{\ln 2}]. \quad (55)$$

The critical mutation probability reaches its maximal value $\mu_c = 1/2$ at the value $\kappa_c = 2\sqrt{\ln 2}$ of the inverse selective temperature, which coincides with the glass transition of the REM [65]. For $\kappa > \kappa_c$ the selective advantage of the most fit sequence is so great that it dominates the population even in the limiting case $\mu = 1/2$, when a complete reshuffling of genotypes occurs in each generation.

We note that, in contrast to most examples discussed in Sect. 3, the expression (55) is independent of the sequence length N . This is a consequence of the scaling of the random energies in (54). Indeed, this scaling implies that the ratio $W_{\max}/W_{\min} = \exp[2E_{\max}]$ grows exponentially in N , and hence the right hand side of (38) is independent of N .

4.3 Correlated landscapes

An example of a random fitness landscape with correlations can be constructed from the Sherrington-Kirkpatrick (SK) spin glass model, which is defined by the energy function

$$E_{\text{SK}}(\sigma) = \frac{1}{N} \sum_{i < j} J_{ij} \sigma_i \sigma_j. \quad (56)$$

Here $\sigma_i = \pm 1$ and the J_{ij} are independent Gaussian random variables with zero mean and unit variance. A similar energy function arises for the graph bipartitioning problem (GBP) discussed in Sect. 2.1,

$$E_{\text{GBP}}(\sigma) = - \sum_{i < j} J_{ij} \sigma_i \sigma_j, \quad (57)$$

where the spins satisfy the vanishing total spin constraint. In this case $J_{ij} = J > 0$ if the sites i and j are connected by an edge of the graph, and $J_{ij} = 0$ else [22, 42]. Through (53) energy functions (56) and (57) can be directly interpreted as Malthusian fitness landscapes [58, 66, 42]. They belong to a large class of random landscapes for which the correlation function behaves as [60]

$$\rho(d, N) \approx 1 - a_1 \frac{d}{N} + \mathcal{O}\left(\left(\frac{d}{N}\right)^2\right) \quad (58)$$

for $N, d \rightarrow \infty$ but $d/N \ll 1$, with a constant a_1 which is independent of N . The significance of this behavior becomes clear if we interpret d/N as a continuous variable: For random functions of a real variable, the linear dependence of the correlation function for small arguments is typical of a non-differentiable process with independent increments (such as Brownian motion), whereas for a differentiable random process the correlation function varies quadratically at small distances. In this sense the linear behavior in (58) is indicative of the ruggedness of the landscape.

A simple modification of the argument leading to (55) gives some insight into how the fitness correlations affect the location of the error threshold [42]. We assume that in the localised phase the bulk of the population is located at some distance $d^* = \mathcal{O}(1)$ from the most fit genotype σ_{max} , with corresponding energy values $\bar{E} \approx \rho(d^*)E_{\text{max}}$. Equating the resulting mean population fitness $\bar{W} = \exp[\kappa \bar{E}]$ to the product $(1 - \mu)^N W_{\text{max}}$ and using (58) then yields, for large N , the estimate

$$\mu_c \approx \frac{\kappa a_1 d^* E_{\text{max}}}{N^2}. \quad (59)$$

Together with the scaling of the ground state energy as $E_{\text{max}}^{\text{SK}} \sim N^{1/2}$ and $E_{\text{max}}^{\text{GBP}} \sim N^{3/2}$ for the SK-model and the GBP, it follows that $\mu_c^{\text{SK}} \sim N^{-3/2}$ and $\mu_c^{\text{GBP}} \sim N^{-1/2}$, respectively, in agreement with simulations [42].

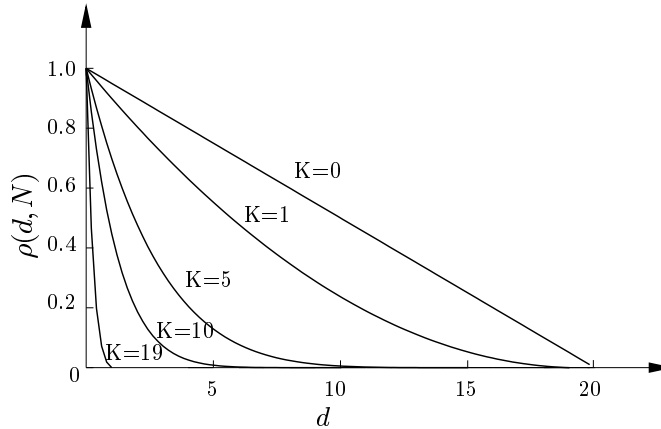


Fig. 5. Correlation function (61) for the NK -model with $N = 20$.

A family of random landscapes in which the ruggedness can be tuned are the NK landscapes⁹ introduced by Kauffman and Levin [5, 68]. In this model, the Malthusian fitness¹⁰ of a genotype is written as a sum of contributions from the N loci,

$$w(\sigma) = \frac{1}{N} \sum_{i=1}^N w_i, \quad (60)$$

where each w_i is a function of σ_i and K other loci chosen at random¹¹. The number of possible states of σ_i and its K chosen neighbors is then ℓ^{K+1} , and each of these states is assigned a random fitness drawn from some continuous probability distribution. For large N the additive form of (60) ensures that the $w(\sigma)$ become Gaussian by virtue of the central limit theorem.

For $K = 0$ the loci are independent, and the model becomes equivalent to the multiplicative fitness landscape without epistasis discussed in Sect. 3.4; in particular, there is a unique fitness peak. At the other extreme $K = N - 1$, the w_i are independent random variables and the model reduces to the uncorrelated landscape of Sect. 4.2. With increasing K the number of fitness maxima increases and their height decreases [68], and the correlation function is given by¹² [71]

⁹ A related family was defined in [66] in analogy to Derrida's p -spin model of spin glasses [65].

¹⁰ A Wrightian version of the model is discussed in [69].

¹¹ Other schemes for choosing the interacting loci are described in [17, 60, 69].

¹² The expressions for the correlation function given in [60, 70] are incorrect, because it is not taken into account that the d mutations separating the two genotypes in (51) must affect different sites in the sequence.

$$\rho(d, N) = \begin{cases} \frac{(N-K-1)! (N-d)!}{N! (N-K-d-1)!} & : d \leq N - K - 1 \\ 0 & : \text{else.} \end{cases} \quad (61)$$

This shows how the correlations decay more rapidly with increasing epistasis (increasing K), and reduces to $\rho(d, N) = 1 - d/N$ for $K = 0$ and $\rho(d, N) = \delta_{d,0}$ for $K = N - 1$, respectively (see Fig. 5).

Another model with tunable correlations was introduced in a study of evolutionary dynamics in the limit of infinite genome size but with a finite population [72]. For $N \rightarrow \infty$ every mutation creates a genotype that has not been previously represented in the population. The fitnesses can then be created “on the fly” according to the transition probability

$$\text{Prob}[w(\sigma)|w(\sigma')] \sim \exp[-(w(\sigma) - \lambda^d w(\sigma'))^2] \quad (62)$$

where $d = d(\sigma, \sigma')$ and the parameter $0 \leq \lambda \leq 1$ determines the decay of the correlations as $\rho(d, N) \sim \lambda^d$.

4.4 Neutrality

We have seen above in Sect. 4.1 that realistic fitness landscapes obtained from mapping sequences to structures contain extended regions that are selectively neutral. It has been argued that this is a general feature of high-dimensional fitness landscapes, which has important consequences for the way in which evolutionary dynamics should be visualized [2]. Rather than consisting of valleys and hilltops, as suggested by the low-dimensional rendition in Fig. 4, such a *holey landscape* would display a network of ridges of approximately constant fitness, along which a population can travel large genetic distances without ever having to cross an unfavorable low-fitness region¹³.

Several properties of the stationary population distribution for the quasispecies model on a neutral network can be inferred without specifying the precise structure of the network [73]. It is only assumed that the viable genotypes make up a connected graph \mathcal{G} of constant fitness, which is surrounded by genotypes that are lethal or at least of very low fitness. Mutations are restricted to nearest neighbor sequences. Then the key observation is that the stationary population distribution $X(\sigma)$ on the network¹⁴ is the principal

¹³ The evolutionary importance of paths of viable genotypes that connect distant points in sequence space was emphasized by Maynard Smith [3]. He illustrates the issue with a game where the goal is to transform one word into another by changing one letter at a time, with the requirement that all intermediate words are meaningful (i.e., “viable”). An example is the path WORD \rightarrow WORE \rightarrow GORE \rightarrow GONE \rightarrow GENE.

¹⁴ The population on the network is normalized to unity, $\sum_{\sigma \in \mathcal{G}} X(\sigma) = 1$, which does not include the individuals in the lethal region. Although these individuals do not reproduce, they constitute a finite fraction of the population which is replenished by mutations from viable genotypes.

eigenvector of the *adjacency matrix* of the graph, which is a matrix that has unit entries for pairs of viable sequences that are connected by a single point mutation, and zero entries otherwise. The corresponding eigenvalue Λ is equal to the *population neutrality* $\langle \nu \rangle$,

$$\Lambda = \langle \nu \rangle = \sum_{\sigma \in \mathcal{G}} \nu(\sigma) X(\sigma), \quad (63)$$

where $\nu(\sigma)$ is the number of viable neighbors of sequence σ (the *degree* of the corresponding node of \mathcal{G}). The weighting by the population fraction $X(\sigma)$ in (63) is significant: For any graph \mathcal{G} the principal eigenvalue of the adjacency matrix satisfies the bounds [75]

$$\bar{\nu} \leq \Lambda \leq \nu_{\max}, \quad (64)$$

where $\bar{\nu}$ and ν_{\max} denote the average and maximal degrees of the graph. For a random graph with a range of degrees the relations (63) and (64) imply that generally $\langle \nu \rangle > \bar{\nu}$, which shows that the population preferentially resides at nodes where the number of viable neighbors is larger than on average. This has been referred to as the evolution of *mutational robustness* [73]. The heterogeneity of the node degree along the neutral network has important consequences also for the evolutionary dynamics, because it induces strong fluctuations in the rate of neutral substitutions [63, 64, 74].

Neutral networks can be modeled as random subgraphs in sequence space. Such subgraphs are defined through a simple modification of the uncorrelated landscape model of Sect. 4.2, where each sequence σ is randomly assigned fitness $W(\sigma) = 1$ (*viable*) with probability P and $W(\sigma) = 0$ (*lethal*) with probability $1 - P$. Each connected region of viable genotypes then constitutes a random subgraph. For small P these regions are small and isolated, but at the *percolation threshold* $P = P_c$ given by

$$P_c = \frac{1}{(\ell - 1)N} \quad (65)$$

a giant network appears which spans the sequence space and which, for $P > P_c$, contains a finite fraction of all sequences [2, 76]. Since N is a large number, the fraction of viable genotypes needed to create such a spanning network is remarkably small [3].

For subgraphs of the binary hypercube ($\ell = 2$) with random assignment of links (rather than sites) it has been shown that the principal eigenvalue of the adjacency matrix is asymptotically given by [75]

$$\Lambda \approx \max[NP, \sqrt{\nu_{\max}}]. \quad (66)$$

Taking $N \rightarrow \infty$ at fixed P one finds that $\nu_{\max} \sim N$, so that $\Lambda \rightarrow NP = \bar{\nu}$. In this limit the neutral network behaves like a regular graph, and no significant mutational robustness develops. On the other hand, if $P \rightarrow 0$ as $N \rightarrow \infty$ with NP fixed, one obtains $\nu_{\max} \sim N/\ln N \gg \bar{\nu}$, and the mutational robustness effect is significant.

5 Dynamics of adaptation

In this section we turn our attention to time-dependent aspects of the adaptive process. In rugged fitness landscapes the population is faced with the task of reaching ever higher fitness peaks by traversing fitness valleys or neutral networks, which typically gives rise to a pattern of episodic or *punctuated* evolution. This phenomenon will be discussed in general terms in the following subsection, and a specific model study [77] will be summarized in Sect. 5.2. In the final subsection we describe an approach to evolutionary dynamics that is suited for landscapes that are *smooth*, in the sense that a simple (linear) relation between fitness and genetic distance can be assumed.

5.1 Peak shifts and punctuated evolution

The existence of multiple fitness peaks of different height, as illustrated in Fig. 4, immediately suggests that evolutionary histories should generally display two distinct regimes: Periods of stabilizing selection, where the population resides near a local fitness maximum, and *peak shifts* in which the population moves quickly from one fitness peak to another of greater height. The stationary distributions in a single peak landscape that were discussed at length in Sect. 3 can be viewed as an approximate description of the first regime. The necessity of peak shifts for explaining the succession of biological forms in the paleontological data has been recognized for a long time¹⁵, but the underlying mechanisms (and even the relevance of the concept itself) remain controversial.

Mathematical analysis of peak shifts driven by stochastic fluctuations in finite populations (genetic drift) generally show that the waiting time for the shift is vastly larger than the time required for the transition itself [79, 80]. This can be argued to support the scenario of *punctuated equilibrium* in macroevolution [81], which states that evolutionary changes (including both speciation and phenotypic changes within a lineage) occur during relatively short time intervals which are separated by long periods of no discernible change (*stasis*).

However, for realistic population sizes the stochastically driven peak shifts may be far too rare to be relevant, and in fact they may not be needed at all, if the picture of a holey landscape spanned by a network of neutral ridges described in Sect. 4.4 is generally applicable [2]. Evolution in such a landscape will nevertheless be punctuated, because a population moving by genetic drift across a neutral network can increase its fitness only by finding a path to another network of higher fitness. If these paths are rare, a natural separation of time scales between (phenotypic) stasis and sudden fitness jumps arises. This scenario is well established for simulations of *in vitro* evolution of RNA

¹⁵ A famous example is the transition from browsing to grazing behavior in equids [78].

sequences [20, 82]. Borrowing a concept from statistical physics, it can be said that in this case the population is confined by *entropic* barriers rather than by fitness barriers [83].

5.2 Evolutionary trajectories for the quasispecies model

In the deterministic mutation-selection models of interest in this chapter, stochastic fluctuations cannot be invoked to drive peak shifts. Nevertheless a population initially placed near one fitness peak in a multi-peaked landscape is able to relocate to a higher peak, by developing tails of mutants which (since the number of individuals is formally infinite) with time explore the entire sequence space. Once a small mutant population has been established at the distant fitness peak, it starts to compete with the majority at the original peak and, if the newly populated peak is higher, it will eventually come to dominate the population. In this way the majority of the population can shift between peaks without ever actually having to traverse a fitness valley (Fig. 6).

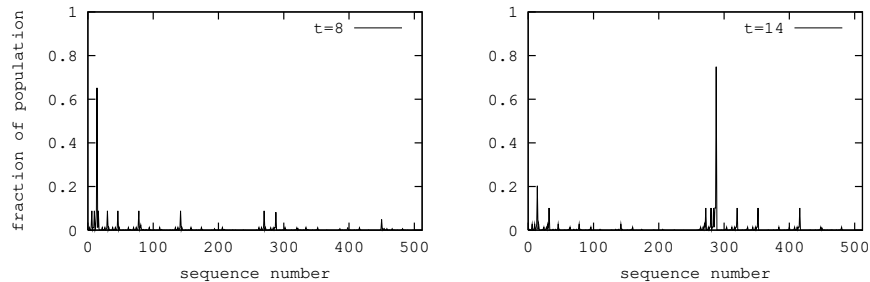


Fig. 6. Example of a peak shift event for quasispecies dynamics with binary sequences of length $N = 9$ in an uncorrelated random fitness landscape. At time $t = 8$ the most populated sequence is near the origin (sequence number 1), but at time $t = 14$ it has moved to a sequence number close to 300. The peaks of lower height represent the first- and second neighbor mutants of the most populated sequence. They are not adjacent because of the linear arrangement of the sequences.

The time t_x required for a single peak shift in the discrete time quasispecies model has been estimated numerically for a simple degenerate two-peak landscape, given by (32) with $W_N = W_0$ and $W_{N-1} = 1$ [84]. The population was first allowed to equilibrate in a single peak landscape and then the second peak was turned on. The result is

$$t_x \sim \left(\frac{\ln W_0}{N\mu} \right)^N \sim \left(\frac{\mu_c}{\mu} \right)^N \quad (67)$$

which, somewhat surprisingly, has the same form as the time required for a finite population to cross a fitness valley [83]; of course in the latter case there is an additional dependence on the population size.

The evolutionary trajectories that result from multiple peak shifts in an uncorrelated rugged fitness landscape have been studied in detail in a strong selection limit motivated by the zero temperature limit of the statistical physics of disordered systems [77, 85, 86, 87]. Writing

$$Z(\sigma, t) = e^{\kappa F(\sigma, t)}, \quad W(\sigma) = e^{\kappa E(\sigma)}, \quad \mu = e^{-\kappa}, \quad (68)$$

with κ denoting the inverse selective temperature (see Sect. 4.2), and starting with an initial condition $Z(\sigma, 0) = \delta_{\sigma, \sigma^{(0)}}$ where $\sigma^{(0)}$ is a randomly chosen sequence, the dynamics takes the following form in the $\kappa \rightarrow \infty$ limit:

$$F(\sigma, t+1) = \max_{\sigma'} [F(\sigma', t) + E(\sigma') - d(\sigma, \sigma')], \quad t \geq 2 \quad (69)$$

$$F(\sigma, 1) = E(\sigma^{(0)}) - d(\sigma, \sigma^{(0)}). \quad (70)$$

Here the logarithmic fitnesses $E(\sigma)$ are independent random variables chosen from a common distribution $p(E)$. As already discussed in Sect. 4.2, one expects the whole population to be localised at the fittest genotype in the large time limit. At any finite time, in the strong selection limit, the population can be identified with the most populated genotype. The behavior of this genotype is essentially unaffected by dropping the mutation term for times $t > 1$, so that the dynamics reduces to [86]

$$F(\sigma, t) = F(\sigma, 1) + (t-1)E(\sigma), \quad t \geq 2. \quad (71)$$

This illustrates the fact that, after the entire sequence space has been “seeded” by mutants of the original genotype $\sigma^{(0)}$ at time $t = 1$, the subsequent evolution consists in the competition of independent populations located at the fitness peaks. Distant peaks of high fitness are disadvantaged by a small initial population but may come to dominate at later times.

Since the seeding population $F(\sigma, 1)$ of a sequence only depends on its distance from the initial genotype $\sigma^{(0)}$, within each *shell* of constant $k = d(\sigma, \sigma^{(0)})$ only the most fit genotype is a contender for global leadership. Thus the dynamics of the ℓ^N variables (71) can be reduced to $N+1$ shell population variables $F(k, t)$ whose fitnesses $E(k)$ are chosen from the distribution

$$p_k(E) = \alpha_k p(E) \left(\int_{E_{\min}}^E p(x) dx \right)^{\alpha_k - 1}. \quad (72)$$

This is the distribution of the maximum among α_k independent random variables with distribution $p(E)$, and α_k is the number of sequences in shell k , as defined in (4).

The representation of the “evolutionary race” as a problem of crossing straight lines¹⁶ is illustrated in Fig. 7. At a given time t , the most populated

¹⁶ The problem is related to models of highway traffic, where each vehicle is equipped with a fixed random speed and overtaking is forbidden [88].

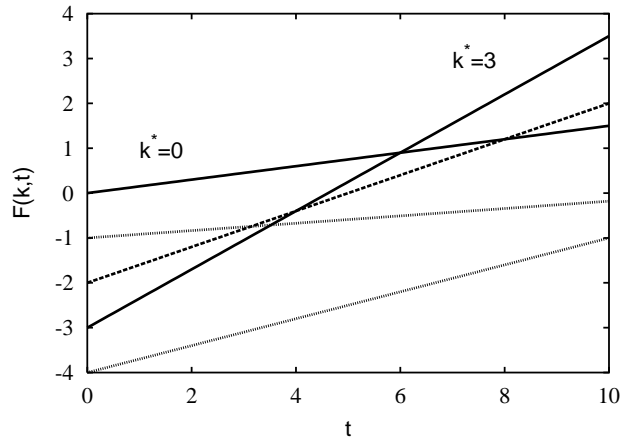


Fig. 7. Illustration of the linear dynamics (71). For each shell of constant Hamming distance k from $\sigma^{(0)}$ only the line with the largest slope is drawn. Dashed lines are fitness records, dotted lines are non-records, and solid lines are records that are not bypassed.

sequence located in shell k^* leads until it is overtaken by a shell $k^{*'}$ with $E(k^{*'}) > E(k^*)$ and so on, until the global fitness maximum takes over. A natural question of interest is to identify the sequences that take part in this evolutionary trajectory, and to determine their number. It is clear that for a sequence to participate in the trajectory it is necessary that it constitutes a *fitness record*, in the sense that its fitness exceeds the fitnesses of all sequences that are closer to $\sigma^{(0)}$. An analytical treatment of the statistics of these independent but non-identically distributed records shows that the average number of records encountered on the way to the global maximum is [77]

$$\mathcal{R} \approx \frac{(\ell - \ln \ell - 1)}{\ell - 1} N \quad (73)$$

for large N , and that essentially all records are located within the distance $d_{\max} = N(\ell - 1)/\ell$ near which most of the sequences (including the most fit sequence) reside. For $\ell = 2$, the inter-record spacing between the j -th and $j + 1$ -th record is of the order \sqrt{N}/j where $j = 1$ labels the last record (the global maximum). Thus, a few records separated by distances of order \sqrt{N} occur near d_{\max} and the rest are clustered away from it.

However, many records are *bypassed* by fitter sequences that arise further away from $\sigma^{(0)}$ but manage to catch up with the current leader at an earlier time. For unbounded fitness distributions with Gaussian or exponential tails, the number of non-bypassed records (which is the number of sequences that take part in a trajectory) is found to be only of order \sqrt{N} with a uniform spacing $\sim \sqrt{N}$, which suggests that the competition among the contenders is

strong when the average fitness of the population is still low. For fat-tailed power law distributions the average number of records that are not bypassed is asymptotically equal to unity, which implies that the population relocates to the global fitness maximum in a single step.

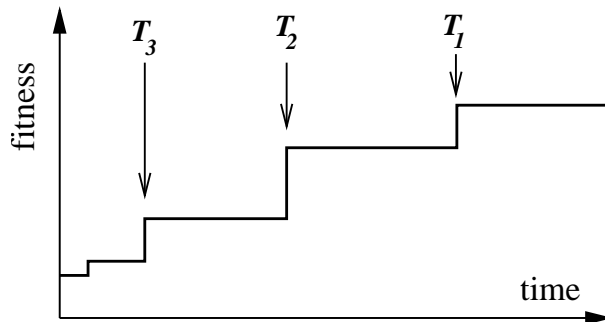


Fig. 8. Timing of evolutionary jumps.

Several statistical properties of the *timing* of peak shifts turn out to be independent of the fitness distribution $p(F)$ [77, 85, 86]. Specifically, denoting by T_j the time at which the j th peak shift occurs, with $j = 1$ denoting the last shift (which reaches the global fitness maximum), $j = 2$ the penultimate peak shift and so on (Fig. 8), the corresponding distributions display universal power law tails

$$P_j(T_j) \sim (T_j)^{-(j+1)}. \quad (74)$$

In particular, the expected value of T_1 is infinite. The prefactors of these power laws depend however on the fitness distribution and the sequence length, in such a way that e.g. the typical value of T_1 tends to unity for fitness distributions with a power law tail.

5.3 Dynamics in smooth fitness landscapes

So far we have discussed landscapes in which the fitnesses can be very different from each other and as described above, the evolutionary trajectory can change in a stepwise manner if the landscape has local maxima. Smoothly varying landscapes for which the system does not get trapped in such metastable states are the subject of the following discussion. *Smoothness* will be taken to imply here that there is a simple (linear) relationship between the fitness of a genotype and its genetic distance from the master sequence. Individuals can then be characterized by their fitness alone, and the description can be based on a one-dimensional *fitness space* [89].

The prototypical case in which this reasoning applies is that of the multiplicative fitness landscape discussed in Sect. 3.4. We work in the Malthusian

setting and assume that the fitness $w(\sigma)$ is simply equal to the number of mismatches with respect to the master sequence, $w = 0, \dots, N$. Then the fraction $Y(w, t)$ of individuals with fitness w at time t evolves as [89]

$$\begin{aligned} \dot{Y}(w, t) = & (w - \bar{w})Y(w, t) + \\ & + \tilde{\mu}[(w + 1)Y(w + 1, t) + (N - w + 1)Y(w - 1, t) - NY(w, t)], \end{aligned} \quad (75)$$

which is just the paramuse equation (7) evaluated for the present fitness landscape, with \bar{w} denoting the mean fitness of the population. For large N the fitness w can be treated as a continuous variable. Setting $r = (w - N/2)/\sqrt{N}$, $\bar{\mu} = \tilde{\mu}/\sqrt{N}$ and $\tau = \sqrt{N}t$, Eq. (75) reduces for $N \rightarrow \infty$ to the drift-diffusion equation

$$\frac{\partial Y}{\partial \tau} = (r - \bar{r})Y + \frac{\bar{\mu}}{2} \frac{\partial^2 Y}{\partial r^2} + \frac{\partial}{\partial r}(2\bar{\mu}rY). \quad (76)$$

Analysis of (75, 76) and related equations [90] shows that the mean fitness diverges in finite time, since the equations ignore the fact that at least one individual is required to initiate the reproduction process. This can be circumvented by imposing a cutoff Y_c inversely proportional to the population size, below which the selection term does not operate.

With this modification, one finds that at short times, the population which was initially spread over a fitness range gets localised about the maximum available fitness leading to a fast growth of average fitness. This is followed by the collective motion of the localised ‘‘species’’ as a traveling wave with constant speed and width (as long as the population is far from the boundaries $w = 0$ and N of the fitness space). A finite population size analysis of discrete models (described in the infinite population limit by the above continuum equations) shows that both speed and variance of the wave diverge linearly with increasing population size, which is consistent with the finite time singularity that appears in the absence of a cutoff [90].

Quantitative agreement with finite population simulations requires a more careful treatment in which the most fit non-empty mutant class is treated stochastically, while keeping deterministic differential-difference equations of the type (75) for the remainder of the population. In addition, the continuum limit of (75) should be carried out on the level of $\ln Y$ rather than for Y itself, which leads to a nonlinear drift-diffusion equation replacing (76) [27]. Recent applications of fitness space models that go beyond the present discussion include studies of the *in vitro* evolution of DNA sequences selected for protein binding [46], viral populations undergoing serial population transfers [91], and the effects of recombination in asexual populations [92].

6 Evolution in the laboratory

Viruses and bacteria are suitable candidates for testing the theory of asexual evolution due to their simple genomes and high replication rates. For instance,

RNA viruses which are characterised by high mutation rates and small genome (see Table 2.1 and the chapter by E. Lázaro in this book) can produce about 10^4 copies an hour. Their typical population numbers are of the order of 10^{11} , thus getting close to the infinite population condition for the applicability of quasispecies theory. Interestingly, evolution can also occur in non-living systems such as RNA extracted from a bacteriophage which we now proceed to discuss in the following subsection.

6.1 RNA evolution *in vitro*

Early *in vitro* studies of adaptation to a given environment were carried out on a simple system comprising of RNA molecules and the enzyme RNA replicase which is required to catalyse the RNA replication reaction. In the first of a series of experiments, the time interval during which the reaction is allowed to proceed was gradually reduced with the number of generations, thus selecting the rapidly growing molecules [93]. By the 74th generation, the initial baseline strain with a genome length of a few thousand bases evolved to a 15 times faster replicating (but no longer pathogenic) chain of merely a few hundred bases, by casting off the parts of the genome which do not participate in the *in vitro* replication process. Subsequently, experiments using such short RNA were performed under different conditions and selection pressure [94, 95]. In particular, the formation of a quasispecies consisting only to 40% of the master sequence and many mutants has been demonstrated [96].

6.2 Quasispecies formation in RNA viruses

Inside a cell, a virus is subjected to the constantly changing environment of the host, whereas the quasispecies concept described in earlier sections assumes an infinite population evolving towards a stationary state in a static landscape. Nevertheless, evidence for quasispecies formation has been obtained in *in vivo* experiments on RNA viruses by examining their genetic heterogeneity [97], and the quasispecies concept now plays an important role in virology [98, 99, 100]; for a detailed discussion we refer to the chapter by Ester Lázaro in this book.

The first such experiment was performed on a $Q\beta$ phage population derived from the wild type [25]. On sampling about 10% of its sequence, it was found that on average, the genome of the derived phage differs from the wild type at about two positions. Assuming a Poisson model for the distribution of deviations from the wild type, only 14% of the population was found to be wild type and the rest was accounted for by related mutants with up to 3-4 substitutions. Similarly, in the Hepatitis C virus, half of the RNA molecules were found to be identical and the rest one to four mutations away from each other [101]. In the case of HIV, the quasispecies concept has been used to explain the reappearance of the virus after the treatment with drugs that target only the wild type [102]. Many experiments, such as [103] on poliovirus,

also show that RNA viruses operate close to the error threshold, since on a modest increase in mutation rate (through chemicals), the virus population was found to lose its genetic structure.

6.3 Dynamics of microbial evolution

The dynamics of adaptation have been studied in several long-term experiments on asexually reproducing microbes like viruses and bacteria. In experiments on *E. coli* [104, 105], several populations are derived from the same ancestor and allowed to replicate under identical conditions. The ancestor is engineered to have a selectively neutral marker so that it can be distinguished from the offspring colony. The process of evolution occurs because the progeny is grown in the presence of limited supply of glucose, unlike the ancestor.

To measure the fitness of the evolved type, the ancestor and the evolved progeny are made to compete for glucose by mixing them in equal amounts at time $t = 0$ and estimating their respective densities ρ_A and ρ_P at $t = 0$ and $t = 1$ where time is measured in days. Then the Malthusian fitness of the evolved type at any instant measured relative to the ancestor A is given by

$$w = \frac{\ln(\rho_P(1)/\rho_P(0))}{\ln(\rho_A(1)/\rho_A(0))}. \quad (77)$$

The experiments indicate that the fitness of all populations improves in time, but each of the replicate populations reaches a different fitness level at large times. This supports the picture of a rugged fitness landscape (Fig. 4) with several peaks in which the population, starting from the same initial point, reaches different local maxima via different evolutionary trajectories.

Initially fitness changes rapidly but slows down considerably in the course of time. When the same experimental data is viewed at a finer scale, the best fit to the data is obtained if the fitness increases are assumed to occur in steps. The occurrence of punctuated evolution is associated with the selection of rare beneficial mutations [106]. Although a large number of advantageous mutations with small effects may have occurred, a few mutations with large effects quickly spread through the population and are responsible for the jumps in the fitness. For a review of other experiments with this bacterial population see [9, 107].

The step-like nature of fitness trajectories, especially the properties of the first step, has been investigated in detail in other experiments as well. For instance, in [108], the distribution of the fitness conferred in the first step was measured in *E. coli*, which supports the above observation of the occurrence of few mutations with large benefits and many with small payoffs. Similar experiments have also been performed on the RNA virus ϕ_6 [109]. This study tracked the fitness recovery in a population, after a deleterious mutation has been induced by a population bottleneck, for about hundred generations. The fitness was seen to recover in steps but the number of steps (and the fitness

benefit) was found to depend strongly on the population size. While large populations recovered in one large step, smaller populations required many steps each granting small favors. As discussed in detail in the chapter by Ester Lázaro, such population bottlenecks occur naturally in the life cycle of viruses, because the number of viral particles that are transmitted from one host to another is often very small.

Finally, we note that under certain conditions populations of RNA viruses display a linear increase or decrease of fitness with time [27, 110], which can be analyzed within the framework of the fitness space models discussed in Sect. 5.3.

7 Conclusions

In this chapter we have given an overview over a class of models of adaptive evolution which include selection and mutation, but (due to their deterministic character) ignore effects of genetic drift in finite populations. A large body of work spread out over different scientific communities has been devoted to such models, and our survey must necessarily remain quite incomplete. We have therefore tried to focus on some general concepts – such as sequence space, fitness landscapes, error thresholds and epistatic interactions – that we believe to be useful also beyond the specific biological situations in which the models apply.

Stochastic effects characteristic of finite populations are expected to be quantitatively and even qualitatively important for several of the phenomena we have described. Genetic drift induces a new mechanism of genetic degradation, *Muller's ratchet* [111], in which the fittest genotype is lost from the population because it is not sampled for reproduction. In the limit of infinite sequence length this process is irreversible, and it generally contributes to the delocalisation of the population from fitness peaks. Correspondingly, a common result of finite population studies in simple [23, 37, 48] as well as complex [42, 72] landscapes is a lowering of the error threshold mutation rate with decreasing population size. A comparison between Muller's ratchet and the error threshold in infinite population models can be found in [10, 50]. As described in the chapter by E. Lázaro, both mechanisms for genetic degradation are being considered as possible strategies for fighting viral infections.

The finite size of the population is also crucially important for the peak shifts in rugged landscapes discussed in Sect. 5.2, because it imposes a cutoff on the tails of rare mutants which are responsible for the communication between distant fitness peaks. Much of the analytic work on adaptive dynamics that takes stochastic aspects into account has considered the regime of low mutation rates¹⁷, where the population consists of a single genotype at most

¹⁷ The quantitative characterization of this regime is that the product of the population size and the mutation probability per site is small compared to unity [26].

times and the generation and fixation of new mutations are rare events. In these studies the geometrical constraints on the availability of new mutants in sequence space are usually ignored, and the timing and fitness effects of mutations are instead generated by a suitable stochastic process [112, 113]. An important task for the future will be to integrate the different theoretical approaches, with the ultimate goal of bringing them to bear on the experimental data that are becoming available.

Acknowledgements

This work was supported by DFG within SFB-TR12 *Symmetries and universality in mesoscopic systems*. JK is grateful to E. Ben-Naim, D. Krakauer, H. Levine and T. Wiehe for useful discussions, and to the Laboratory of Physics of HUT for the kind hospitality during the completion of the article.

References

1. S. Wright, *Proceedings of the 6th International Congress of Genetics I* 356 (1932).
2. S. Gavrillets, *Fitness Landscapes and the Origin of Species* (Princeton University Press, 2004).
3. J. Maynard Smith, *Nature* **225** 563 (1970).
4. M. Eigen, *Naturwissenschaften* **58** 465 (1971).
5. S. Kauffman, S. Levin, *J. theor. Biol.* **128** 11 (1987).
6. J. F. Crow, M. Kimura, *An Introduction to Population Genetics Theory* (Harper and Row, New York, 1970).
7. M. Travisano, *Curr. Biol.* **11** R440 (2001).
8. H.A. Orr, *Nature Review Genetics* **6**, 119 (2005).
9. S. F. Elena, R. E. Lenski, *Nature Reviews Genetics* **4** 457 (2003).
10. E. Baake, W. Gabriel, *Annu. Rev. Comput. Phys.* **7** 203 (2000).
11. E. Baake, H. Wagner, *Genet. Res. Camb.* **78** 93 (2001).
12. B. Drossel, *Adv. Phys.* **50** 209 (2001).
13. L. Peliti, in *Physics of Biomaterials: Fluctuations, Self-Assembly and Evolution*, ed. by T. Riste and D. Sherrington (Kluwer, Dordrecht, 1996), p. 267.
14. L. Peliti, [cond-mat/9712027](https://arxiv.org/abs/cond-mat/9712027).
15. R. Bürger, *Genetica* **102/103** 279 (1998).
16. U. Gerland, T. Hwa, *J. Mol. Evol.* **55** 386 (2002).
17. A. S. Perelson, C. A. Macken, *Proc. Natl. Acad. Sci.* **92** 9657 (1995).
18. C. O. Wilke, C. Adami, *Trends Ecol. Evol.* **17** 528 (2002).
19. P. F. Stadler, in *Biological Evolution and Statistical Physics*, ed. by M. Lässig and A. Valleriani (Springer, Berlin 2002), p. 183
20. P. Schuster, in *Biological Evolution and Statistical Physics*, ed. by M. Lässig and A. Valleriani (Springer, Berlin 2002), p. 55.
21. J. W. Drake, B. Charlesworth, D. Charlesworth, J. F. Crow, *Genetics* **148** 1667 (1998).

22. Y. Fu, P. W. Anderson, *J. Phys. A: Math. Gen.* **19** 1605 (1986).
23. T. Wiehe, E. Baake, P. Schuster, *J. theor. Biol.* **177** 1 (1995).
24. D. B. Saakian, C.-K. Hu, *Phys. Rev. E* **69** 046121 (2004).
25. E. Domingo, D. Sabo, T. Taniguchi, C. Weissmann, *Cell* **13** 735 (1978).
26. L. M. Wahl, D. C. Krakauer, *Genetics* **156** 1437 (2000).
27. I. M. Rouzine, J. Wakeley, J. M. Coffin, *Proc. Natl. Acad. Sci.* **100** 587 (2003).
28. P. G. Higgs, *Gen. Res.* **63** 63 (1994).
29. E. Baake, M. Baake, H. Wagner, *Phys. Rev. Lett.* **78** 559 (1997).
30. H. Wagner, E. Baake, T. Gerisch, *J. Stat. Phys.* **92** 1017 (1998).
31. J. Hermisson, H. Wagner, M. Baake, *J. Stat. Phys.* **102** 315 (2001).
32. M. Eigen, P. Schuster, *Naturwissenschaften* **64** 541 (1977).
33. M. Eigen, J. McCaskill, P. Schuster, *J. Phys. Chem.* **92** 6881 (1988); *Adv. Chem. Phys.* **75** 149 (1989).
34. J. B. Kogut, *Rev. Mod. Phys.* **51** 659 (1979).
35. I. Leuthäusser, *J. Chem. Phys.* **84** 1884 (1986); *J. Stat. Phys.* **48** 343 (1987).
36. P. Tarazona, *Phys. Rev. A* **45** 6038 (1992).
37. M. Nowak, P. Schuster, *J. theor. Biol.* **137** 375 (1989).
38. D. S. Rumschitzki, *J. Math. Biol.* **24** 667 (1987).
39. B. Derrida, L. Peliti, *Bull. math. Biol.* **53** 355 (1991).
40. T. Wiehe, *Genet. Res. Camb.* **69** 127 (1997).
41. S. Franz, L. Peliti, *J. Phys. A: Math. Gen.* **30** 4481 (1997).
42. S. Bonhoeffer, P. F. Stadler, *J. theor. Biol.* **164** 359 (1993).
43. S. Galluccio, *Phys. Rev. E* **56** 4526 (1997).
44. L. Peliti, *Europhys. Lett.* **57** 745 (2002).
45. P. Schuster, J. Swetina, *Bull. Math. Biol.* **50** 635 (1988).
46. W. Peng, U. Gerland, T. Hwa, H. Levine, *Phys. Rev. Lett.* **90** 088103 (2003).
47. J. Berg, S. Willmann, M. Lässig, *BMC Evol. Biol.* **4** 42 (2004).
48. G. Woodcock, P. G. Higgs, *J. theor. Biol.* **179** 61 (1996).
49. A. S. Kondrashov, *Nature* **336** 435 (1988).
50. G. P. Wagner, P. Krall, *J. math. Biol.* **32** 33 (1993).
51. E. Baake, T. Wiehe, *J. math. Biol.* **35** 321 (1997).
52. E. Tannenbaum, E. J. Deeds, E. I. Shakhnovich, *Phys. Rev. E* **69** 061916 (2004).
53. M. Nilsson, N. Snaod, *Phys. Rev. Lett.* **84** 191 (2000).
54. C. O. Wilke, C. Ronnewinkel, T. Martinetz, *Phys. Rep.* **349** 395 (2001).
55. M. Nilsson, N. Snaod, *Phys. Rev. E* **65** 031901 (2002).
56. C. O. Wilke, *Phys. Rev. Lett.* **88** 078101 (2002).
57. K. Aoki, M. Furusawa, *Phys. Rev. E* **68** 031904 (2003).
58. P. W. Anderson, *Proc. Natl. Acad. Sci.* **80** 3386 (1983).
59. J.S. McCaskill, *J. Chem. Phys.* **80**, 5194 (1984).
60. W. Fontana, P. F. Stadler, E. G. Bornberg-Bauer, T. Griesmacher, I. L. Hofacker, M. Tacker, P. Tarazona, E. D. Weinberger, P. Schuster, *Phys. Rev. E* **47** 2083 (1993).
61. P. Schuster, W. Fontana, P. F. Stadler, I. L. Hofacker, *Proc. Roy. Soc. Lond. B* **255** 279 (1994).
62. U. Bastolla, H.E. Roman, M. Vendruscolo, *J. theor. Biol.* **200** 49 (1999).
63. U. Bastolla, M. Porto, H.E. Roman, M. Vendruscolo, *J. Mol. Evol.* **56**, 243 (2003).
64. U. Bastolla, M. Porto, H.E. Roman, M. Vendruscolo, *J. Mol. Evol.* **57**, S103 (2003).

65. B. Derrida, Phys. Rev. B **24** 2613 (1981).
66. C. Amitrano, L. Peliti, M. Saber, J. Mol. Evol. **29** 513 (1989).
67. S. Franz, L. Peliti, M. Sellitto, J. Phys. A: Math. Gen. **26** L1195 (1993).
68. S. A. Kauffman, *The Origins of Order* (Oxford University Press, New York 1993).
69. J. J. Welch, D. Waxman, J. theor. Biol. **234** 329 (2005).
70. E. D. Weinberger, Phys. Rev. A **44** 6399 (1991).
71. P. R. A. Campos, C. Adami, C. O. Wilke, Physica A **304** 495 (2002); Erratum **318** 637 (2003).
72. C. O. Wilke, P. R. A. Campos, J. F. Fontanari, J. exp. Zool. (Mol Dev Evol) **294** 274 (2002).
73. E. van Nimwegen, J. P. Crutchfield, M. Huynen, Proc. Natl. Acad. Sci. USA **96** 9716 (1999).
74. U. Bastolla, M. Porto, H.E. Roman, M. Vendruscolo, Phys. Rev. Lett. **89**, 208101 (2002).
75. A. Soshnikov, B. Sudakov, Commun. Math. Phys. **239** 53 (2003).
76. S. Gavrilets, J. Gravner, J. theor. Biol. **184** 51 (1997).
77. K. Jain, J. Krug, J. Stat. Mech. P04008 (2005).
78. G.G. Simpson, *Tempo and Mode in Evolution* (Columbia University Press, New York 1944).
79. C. M. Newman, J. E. Cohen, C. Kipnis, Nature **315** 400 (1985).
80. N. H. Barton, S. Rouhani, J. theor. Biol. **125** 397 (1987).
81. N. Eldredge, *Macroevolutionary Dynamics* (McGraw-Hill, New York 1989).
82. W. Fontana, P. Schuster, Science **280** 1451 (1998).
83. E. van Nimwegen, J. P. Crutchfield, Bull. Math. Biol. **62** 799 (2000).
84. D. Kim, W. Gill, J. Korean Phys. Soc. **44** 973 (2004).
85. J. Krug in *Biological Evolution and Statistical Physics* ed M Lässig and A Valleriani (Springer, Berlin 2002), p. 205.
86. J. Krug, C. Karl, Physica A **318** 137 (2003).
87. J. Krug, K. Jain, Physica A (in press).
88. E. Ben-Naim, P.L. Krapivsky, S. Redner, Phys. Rev. E **50** 822 (1994).
89. L. S. Tsimring, H. Levine, D. A. Kessler, Phys. Rev. Lett. **76** 4440 (1996).
90. D. A. Kessler, H. Levine, D. Ridgway, L. Tsimring, J. Stat. Phys. **87** 519 (1997).
91. S.C. Manrubia, E. Lázaro, J. Pérez-Mercader, C. Escarmís, E. Domingo, Phys. Rev. Lett. **90**, 188102 (2003).
92. E. Cohen, D. A. Kessler, H. Levine, Phys. Rev. Lett. **94** 098102 (2005).
93. D. R. Mills, R. L. Peterson, S. Spigelman, Proc. Natl. Acad. Sci. **58** 217 (1967).
94. C.K. Biebricher, in *Evolutionary Biology*, Vol. 16, ed. by M. Hecht, B. Wallace and G.T. Prance (Plenum Press, New York 1983), pp. 1–52.
95. C. K. Biebricher, W. C. Gardiner, Biophys. Chem. **66** 179 (1997).
96. N. Rohde, H. Daum, C. K. Biebricher, J. Mol. Biol. **249** 754 (1995).
97. E. Domingo, J. J. Holland, Annu. Rev. Microbiol. **51** 151 (1997).
98. M.A. Nowak, R. May, *Virus Dynamics* (Oxford University Press, 2001).
99. M. Eigen, Proc. Natl. Acad. Sci. **99**, 13374 (2002).
100. A. Moya, E. C. Holmes, F. González-Candelas, Nature Reviews Microbiology **2** 279 (2004).
101. M. Martell, J. I. Esteban, J. Quer, J. Genesca, A. Weiner, R. Esteban, J. Guardia, J. Gomez, J. Virol. **66** 3225 (1992).
102. J. M. Coffin, Science **267** 483 (1995).

103. S. Crotty, C. E. Cameron, R. Andino, Proc. Natl. Acad. Sci. **98** 6895 (2001).
104. R. E. Lenski, M. R. Rose, S. C. Simpson, S. C. Tadler, American Naturalist **138** 1315 (1991).
105. R. E. Lenski, M. Travisano, Proc. Natl. Acad. Sci. **91** 6808 (1994).
106. S. F. Elena, V. S. Cooper, R. E. Lenski, Science **272** 1802 (1996).
107. R. E. Lenski, Plant Breeding Reviews **24** 225 (2004).
108. M. Imhof, C. Schlötterer, Proc. Natl. Acad. Sci. **98** 1113 (2001).
109. C. L. Burch, L. Chao, Genetics **151** 921 (1999).
110. I. S. Novella, E. A. Duarte, S. F. Elena, A. Moya, E. Domingo, J. J. Holland, Proc. Natl. Acad. Sci. **92** 5841 (1995).
111. J. Haigh, Theor. Popul. Biol. **14** 251 (1978).
112. H. A. Orr, Genetics **155** 961 (2000).
113. P. Gerrish, Nature **413** 299 (2001).